ORIGINAL RESEARCH

Allogeneic Mesenchymal Stromal Cells Overexpressing Mutant Human Hypoxia-Inducible Factor 1-α (HIF1-α) in an Ovine Model of Acute Myocardial Infarction

Anna P. Hnatiuk, MD, PhD;* Sang-Ging Ong, PhD;* Fernanda D. Olea, PhD; Paola Locatelli, MD, PhD; Johannes Riegler, PhD; Won Hee Lee, PhD; Cheng Hao Jen, BSc; Andrea De Lorenzi, MD; Carlos S. Giménez, MSc; Rubén Laguens, MD, PhD; Joseph C. Wu, MD, PhD; Alberto Crottogini, MD, PhD

***Background*—**Bone marrow mesenchymal stromal cells (BMMSCs) are cardioprotective in acute myocardial infarction (AMI) because of release of paracrine angiogenic and prosurvival factors. Hypoxia-inducible factor 1-α (HIF1-α), rapidly degraded during normoxia, is stabilized during ischemia and upregulates various cardioprotective genes. We hypothesized that BMMSCs engineered to overexpress mutant, oxygen-resistant HIF1-α would confer greater cardioprotection than nontransfected BMMSCs in sheep with AMI.

***Methods and Results*—**Allogeneic BMMSCs transfected with a minicircle vector encoding mutant HIF1-α (BMMSC-HIF) were injected in the peri-infarct of sheep (n=6) undergoing coronary occlusion. Over 2 months, infarct volume measured by cardiac magnetic resonance (CMR) imaging decreased by 71.7±1.3% ($P<0.001$), and left ventricular (LV) percent ejection fraction (%EF) increased near 2-fold ($P<0.001$) in the presence of markedly decreased end-systolic volume. Sheep receiving nontransfected BMMSCs (BMMSC; n=6) displayed less infarct size limitation and percent LVEF improvement, whereas in placebo-treated animals (n=6), neither parameters changed over time. HIF1-α-transfected BMMSCs (BMMSC-HIF) induced angio-/arteriogenesis and decreased apoptosis by HIF1-mediated overexpression of erythropoietin, inducible nitrous oxide synthase, vascular endothelial growth factor, and angiopoietin-1. Cell tracking using paramagnetic iron nanoparticles in 12 additional sheep revealed enhanced long-term retention of BMMSC-HIF.

***Conclusions*—**Intramyocardial delivery of BMMSC-HIF reduced infarct size and improved LV systolic performance compared to BMMSC, attributed to increased neovascularization and cardioprotective effects induced by HIF1-mediated overexpression of paracrine factors and enhanced retention of injected cells. Given the safety of the minicircle vector and the feasibility of BMMSCs for allogeneic application, this treatment may be potentially useful in the clinic. **(*J Am Heart Assoc*. 2016;5:e003714 doi: 10.1161/JAHA.116.003714)**

Key Words: angiogenesis • growth substances • myocardial infarction

Ischemic heart disease remains the leading cause of death and disability worldwide.[1] Its most severe complication, acute myocardial infarction (AMI), results in permanent loss of cardiomyocytes with posterior scar formation, pathological remodeling, and progression to heart failure.[2] Hence, repair and regeneration of cardiac tissue post-AMI has become a key objective of gene- and stem cell–based therapies.

To date, bone marrow mesenchymal stromal cells (BMMSCs) represent the most commonly used cell type in preclinical research and clinical trials. In addition to their ease of isolation

From the Instituto de Medicina Traslacional, Trasplante y Bioingeniería (IMETTYB), Universidad Favaloro-CONICET, Buenos Aires, Argentina (A.P.H., F.D.O., P.L., C.S.G., A.C.); Departamento de Fisiología (A.P.H., F.D.O., P.L., C.S.G., A.C.) and Departmento de Patología (R.L.), Facultad de Ciencias Médicas, Universidad Favaloro, Buenos Aires, Argentina; Stanford Cardiovascular Institute, Stanford University School of Medicine, Stanford, CA (S.-G.O., J.R., W.H.L., J.C.W.); St George's, University of London, United Kingdom (C.H.J.); Departmento de Cardiología, Hospital Universitario de la Fundación Favaloro, Buenos Aires, Argentina (A.D.L.).

Accompanying Videos S1 through S4 are available at http://jaha.ahajournals.org/content/5/7/e003714.full#sec-35

*Dr Hnatiuk and Dr Ong contributed equally to this work.

Correspondence to: Alberto Crottogini, MD, PhD, Department of Physiology, Favaloro University, Solís 453, C1078AAI Buenos Aires, Argentina. E-mail: crottogini@favaloro.edu.ar

Received April 18, 2016; accepted May 28, 2016.

and amplification, BMMSCs display immunomodulation capacity,[3] multilineage potential including differentiation into cardiomyocytes,[4] and ability to release a large number of growth factors involved in neovasculogenesis and myocardial repair.[5] Furthermore, their immune privilege makes them amenable for allogeneic transplantation.[6] Given that BMMSCs are known to exert their beneficial effect mainly through the release of paracrine factors, genetic modifications promoting overexpression of cardioprotective growth factors and signaling molecules may enhance their regenerative potential.[7]

Under hypoxic conditions, HIF1, a basic-helix-loop-helix-PAS heterodimer protein, is a transcriptional activator of a plethora of downstream genes involved in oxygen homeostasis, angiogenesis, cell proliferation and viability, as well as tissue remodeling and erythropoiesis.[8] Its stability and transcriptional activity depend on the intracellular oxygen concentration sensed by the regulatory subunit HIF1-α. During hypoxia, HIF1-α remains stable, but in well-oxygenated conditions, von Hippel-Lindau protein binds to HIF1-α, leading to its ubiquitination and final degradation in the proteasome.[9,10]

Despite being stable in the post-AMI hypoxic environment, HIF1-α progressively declines over the next 2 to 3 days and loses its beneficial effects.[10] Hence, we hypothesized that BMMSCs overexpressing a stable, oxygen-resistant form of HIF1-α may exhibit greater cardioprotective effects than naïve BMMSCs over a 2-month follow-up period. To facilitate potential translation to the clinic, we used a novel nonviral minicircle vector (MC) that displays high transfection efficiency and prolonged transgene expression with the additional advantage of not harboring bacterial sequences typically associated with conventional plasmids.[11]

Methods

All animal procedures were approved by the Institutional Animal Care and Use Committee of Favaloro University (Buenos Aires, Argentina) and performed in accord with the Guide for Care and Use of Laboratory Animals, 8th edition (US National Institutes of Health, 2011).

Isolation and Culture of Ovine BMMSCs

Bone marrow aspirates were aseptically harvested from the iliac crest of donor Corriedale male sheep under general anesthesia (premedication: intramuscular acepromazine maleate 5 mg; induction: intravenous propofol 3 mg/kg; maintenance: 2% isoflurane in oxygen under mechanical ventilation). Bone marrow mononuclear cells were obtained by density gradient centrifugation using Ficoll-Paque Premium (GE Healthcare, Uppsala, Sweden). Isolated cells were cultured in low-glucose (1 g/L) DMEM (Gibco, Carlsbad, CA) supplemented with 1% (vol/vol) Antibiotic-Antimycotic (Gibco) and 20% (vol/vol) FBS (Natocor, Córdoba, Argentina) incubated at 37°C in the presence of 5% CO_2. After 48 hours, nonadherent cells were removed, and BMMSCs were subcultured using TrypLE Express (Gibco) until passage 4 and 70% to 80% confluence for subsequent use in all experiments.

Flow Cytometry Characterization of BMMSCs

BMMSCs were labeled with mouse anti-sheep CD44 (AbDSerotec, Raleigh, NC), mouse anti-human CD166 (BD Biosciences, San Diego, CA), and mouse anti-sheep CD45 (AbDSerotec) and characterized by flow cytometry (FACSCalibur; BD Biosciences, Franklin Lakes, NJ). Sample data were acquired and analyzed using CellQuest-Pro (BD Biosciences) and Cyflogic 1.2.1 software (CyfloLtd, Turku, Finland).

Adipogenic, Chondrogenic and Osteogenic Differentiation

BMMSCs were differentiated into adipocytes, chondrocytes, and osteocytes using the corresponding StemPRO differentiation kits (Gibco), according to the manufacturer's protocols. Histological staining was performed with Oil Red for adipocytes, Alcian Blue for chondrocytes, and Alizarin Red for osteocytes.

Minicircle Vector and Cell Transfection Efficiency

For cell transfection a novel nonviral MC carrying a mutant version of human hypoxia inducible factor 1-alpha (mHIF1-α) was used.[11–13] The construct is based on site-specific mutation of proline 402 and proline 564 (P402A/P564G) preventing O_2-dependent proline hydroxylation and subsequent proteasomal degradation as previously described.[13]

Lipofectamine LTX (2.5 μL; Invitrogen, Carlsbad, CA) and Plus Reagent 2 μL for every 2 μg of MC-DNA were used for transfecting ovine BMMSCs.

Transfection Efficiency

Transfection efficiency was assessed by transfecting BMMSCs with either MC encoding green fluorescent protein (GFP)[14] or a conventional plasmid vector carrying GFP (pCruz GFP; Santa Cruz Biotechnology, Santa Cruz, CA) by flow cytometry analysis on days 1, 3, and 6 post-transfection.

In Vitro Human Mutated HIF1-α Expression

BMMSCs transfected with mHIF1-α as described above (BMMSC-HIF) and naïve BMMSCs (BMMSC) were cultured in

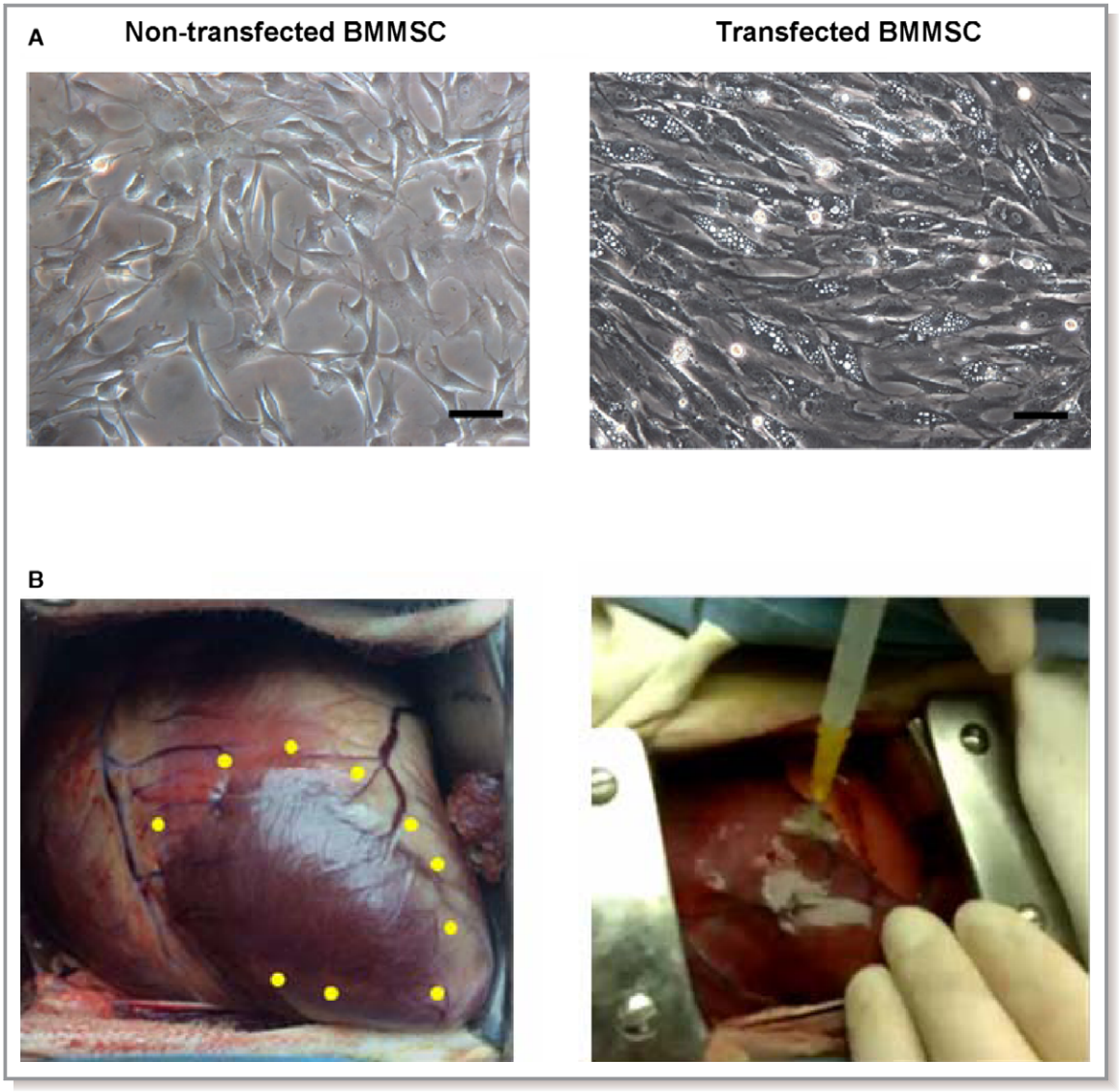

Figure 1. A, Left panel: nontransfected ovine bone marrow mesenchymal stromal cells (BMMSCs) at P4 and 70% confluence. Right panel: HIF1-α-transfected BMMSCs at P4 and 70% to 80% confluence. Bars: 100 μm. B, Left panel: ovine antero-apical infarct (yellow dots indicate injections sites). Right panel: injection procedure in peri-infarct zone using a 1-mL syringe. HIF indicates hypoxia-inducible factor.

6-well dishes (Figure 1A). Cells were lyzed with buffer RTL. Total RNA was extracted using RNeasy mini kit (Qiagen, Hilden, Germany) and reverse-transcription quantitative polymerase chain reaction (RT-qPCR; StepOne Real-Time PCR System; Applied Biosystems, Foster City, CA) was done to quantify mRNA levels of HIF1-α at days 1, 3, and 6 post-transfection. Two sets of primers were used to detect HIF1-α (forward, 5′-CTCAGCCCCAGTGCATTGTA-3′; reverse, 5′-GAA CCTCCTATAGCCACCGC-3′) for wild type and (forward, 5′-TTTACCATGCCCCAGATTCAG-3′; reverse 5′-GGTGAACTTTGTC-TAGTGCTTCCA-3′) for mutant HIF1-α. GAPDH was used as qPCR amplification endogen control (forward, 5′-GGTCGTC TCCTGCGACTTCA-3′ reverse, 5′-GCCCCAGCATCGAAGGT-3′). All primers were designed using Primer Express software (V3.0; Applied Biosystems).

Immunoblotting and In Vitro Hypoxia

BMMSCs were maintained in normoxic conditions or exposed to hypoxic conditions (BD GasPak EZ System; Becton Dickinson) for 24 hours as previously described.[15] Upon completion, cells were washed and lysed for immunoblotting, which was performed with HIF1-α (NB100-105, 1:500; Novus Biologicals LLC, Littleton, CO) and α-tubulin (9099, 1:1000; Cell Signaling Technology, Inc., Danvers, MA). Forty micrograms of proteins were loaded. Expression was normalized to

α-tubulin for whole-cell lysate and densitometry analysis was performed using ImageJ software (National Institutes of Health [NIH], Bethesda, MD).[16]

Surgical Preparation and Study Protocol

Eighteen male Corriedale sheep, weighting 26.7±0.7 kg, were premedicated with intramuscular acepromazine maleate 5 mg. Anesthesia was induced with intravenous propofol 3 mg/kg and maintained with 2% isoflurane in oxygen under mechanical ventilation (Neumovent, Córdoba, Argentina). A sterile thoracotomy was performed at the fourth intercostal space, the pericardium was opened, and an anterior-apical infarct was induced by permanent ligation of branches of the left anterior descending (LAD) coronary artery, avoiding the first diagonal branch (Figure 1B). The LAD itself was not ligated to prevent septal infarction. Thirty minutes after ligation, sheep were randomized into 3 treatment groups (n=6 per group): PBS (placebo group), 2×10^7 nontransfected BMMSCs (BMMSC group), and 2×10^7 HIF1-α-transfected BMMSCs (BMMSC-HIF group). All treatments, diluted in a final volume of 2 mL of PBS, were delivered by direct intramyocardial transepicardial injection, divided into 10 aliquots of 200 μL each. Injections were performed in the normoperfused myocardium surrounding the ischemic area within 5 mm of the infarct border, which was readily visible (Figure 1B) and the needle was retained in the myocardium for 30 seconds after each injection to minimize leakage. The nature of the injections was kept blind for all investigators involved in data analysis and processing. Subsequently, the thoracotomy was repaired without pericardial closure, and, after removal of the tracheal tube, cephalotin 1 g intravenously was injected and sheep were returned to the animal house under analgesic treatment (nalbuphine 0.3 mg/kg, subcutaneous).

Cardiac Magnetic Resonance Procedure

One, 30, and 60 days post-infarction, cardiac magnetic resonance (CMR) imaging was carried out to assess for infarct size and left ventricular (LV) function. CMR was performed with a 1.5 Tesla clinical magnetic resonance scanner (Achieva; Philips, Amsterdam, The Netherlands). To analyze cardiac function, two-dimensional cine steady-state–free precession images with electrocardiogram gating and manual breath hold were acquired in long- and short-axis orientations. A total of 12 to 13 short-axis slices spanning the heart from apex to base and measuring 7 mm in thickness were acquired without gaps using the following imaging parameters: field of view (FOV), 25×25 cm^2; matrix size, 148×120; repetition time (TR), 3.6 ms; echo time (TE), 1.78 ms. To visualize the scar, an intravenous injection of gadolinium-based contrast (0.2 mmol/kg, Dotarem; Temis Lostaló, Buenos Aires, Argentina) was administered and delayed contrast-enhanced images were acquired with a phase-sensitive inversion recovery sequence starting 20 minutes after contrast injection.

The image data for each animal were combined, anonymized, and analyzed with a semiautomated segmentation method[17] using the freely available cardiac analysis software, Segment (version 1.8 R1172; http://segment.heiberg.se). Ischemic initial region and infarct size were expressed as milliliters of infarcted tissue. For cardiac function, LV end-diastolic volume (EDV), end-systolic volume (ESV), and LV percent ejection fraction (%EF) were measured. Long- and short-axis videos of each heart at 1, 30, and 60 days postinjection were recorded.

Short- and Long-Term Cell Tracking

To assess for short-term retention of injected cells, 8 additional sheep were operated as described above and sacrificed 7 days postsurgery. BMMSC and BMMSC-HIF were labeled with Cell Tracker Red CMTPX Dye (Invitrogen) at 0.5-μmol/L concentration in serum-free media according to the manufacturer's protocol and injected in the peri-infarct zone (4 animals per group). Cells were resuspended in PBS after the final washing step for intramyocardial delivery (2×10^7 cells in 2 mL). Myocardial samples from the injected sites were harvested and processed for histological analysis. Given that this short-term tracking yielded positive results (see Results), we decided to measure long-term retention. To this aim, another 8 additional sheep, surgically prepared as described above, were injected in the peri-infarct zones with BMMSC (n=4) or BMMSC-HIF (n=4) labeled as follows: after overnight incubation with 0.1 mg/mL of superparamagnetic iron oxide nanoparticles (SPIO) in low-glucose DMEM (FluidMAG-D; Chemicell, Berlin, Germany), culture plates were washed 3 times with PBS before cells were detached for 3 additional washing steps. Cells for the BMMSC-HIF group were transfected with MC-HIF1-α and 6 hours after transfection labeled with SPIO. After the final washing step, cells were resuspended at a final concentration of 2×10^7 cells in 2 mL of PBS and stored on ice until intramyocardially injected in the peri-infarct zone.

CMR Tracking of Magnetically Labeled BMMSCs

To visualize SPIO-labeled cells, CMR was performed at 1, 30, and 60 days postsurgery with the equipment described above. The T2*-weighted images were acquired using a multiecho gradient echo sequence with the following imaging parameters: FOV, 25×25 cm^2; matrix size, 140×104; TR, 16 ms; and TE, 6.6 ms. The image data for each animal were combined and anonymized for analysis using a manual region-of-interest segmentation method quantifying the volume (mL)

of the hypointensity emitted by the injected zones using Segment software. For all experiments involving SPIO-labeled BMMSCs, 25% labeled cells were mixed with 75% unlabeled cells because iron internalization was sufficient to generate enough CMR signal loss on T2*-weighted images.

Quantification of Myocardial Cell Retention

Cells labeled for 24 hours with FluidMAG-D were washed 3 times, detached, and resuspended in PBS. For T2* measurements, 250 μL of increasing concentration of SPIO-labeled cell suspension (2×10^6–1.25×10^5) were mixed with 250 μL of 2% low-melting-point agarose and filled into 1-mL tubes. Sample tubes were placed into a sample box filled with water to reduce susceptibility effects. Images were performed using a 1.5T clinical magnetic resonance scanner described above. For T2*-weighted images, we used a multiecho gradient echo sequence with the same imaging parameters described previously for CMR tracking of SPIO-labeled BMMSCs in vivo. The number of labeled cells was quantified by measuring hypointense signal of each tube using the free available software, ImageJ (NIH), to estimate the number of cells corresponding to each image's intensity. The calibration curve was performed based on the relation between the number of labeled cells and hypointensity signal and used to estimate the number of retained labeled cells into the myocardial tissue corresponding to hypointense signal emitted in the CMR of each animal at each time point of the follow-up (Figure 2).

Histology

After completing their respective protocols, sheep were premedicated with intramuscular acepromazine maleate (10 mg total) and sacrificed with an overdose of propofol (13–20 mg/kg) followed by an intravenous bolus injection of potassium chloride (60 mEq) to arrest the heart in diastole.

Sheep undergoing the main protocol were sacrificed after the final CMR scanning (60 days post-AMI). The heart was excised, the atria and the right ventricle were removed, and the LV was opened along the posterior interventricular sulcus, extended flat to exhibit its endocardial aspect and photographed. After 24-hour fixation in 4% formaldehyde at room temperature, 2 myocardial samples measuring ≈2 cm^2 (one including the fibrotic scar and the peri-infarct zone and the other only normoperfused tissue remote from the scar) were embedded in paraffin and cut into 4-μm sections. For immunohistochemistry, tissue sections were deparaffinized and brought to PBS solution (pH 7.2). Endogenous peroxidase was blocked with 3% H_2O_2 in methanol, antigens were retrieved with citrate buffer pretreatment in a microwave oven, and sections were incubated during 1 hour with a specific monoclonal antibody against smooth-muscle actin (BioGenex, Fremont, CA) to identify arterioles (vessels measuring 10–100 μm in diameter displaying a smooth-muscle media layer), and the endothelial marker, Biotinylated Euonymous Europaeus Lectin (Vector Laboratories, Burlingame, CA), to identify capillaries (vessels with only an endothelial wall measuring up to 10 μm in diameter). Random fields from the peri-infarct area were examined at ×20 magnification for arterioles and capillaries under light microscopy (Axiophot; Zeiss, Jena, Gremany) with the aid of a computer-assisted image-analysis program (Zeiss AxioCam MRc5 camera and AxioVision software [v4.7.2.0]; Carl Zeiss MicroImaging, Inc., Thornwood, NY). The scanned area was 151.6±23.1 mm^2 for the placebo group, 166.1±22.7 mm^2 for BMMSC, and 173.5±40.8 mm^2 for BMMSC-HIF. Vascular density was expressed as number of capillaries and arterioles per mm^2. In each experimental group, the cross-sectional diameter (CSD; μm) and the lumen diameter (LD; μm) in 20 arterioles per animal were measured at 7 and 60 days. From CSD and LD, wall thickness (WTh; μm) was calculated according to the equation: WTh=(CSD−LD)/2.

Picrosirius red staining was used to quantify fibrosis in normoperfused zones remote from injections sites for the long-term functional protocol hearts. Random fields were examined at ×10. The scanned area was 486.2±91.8 mm^2 for the placebo group, 539.2±113.7 mm^2 for BMMSC, and 432.8±102.7 mm^2 for BMMSC-HIF. All quantifications and images analyses were performed with ImageJ and Image-ProPlus software (v6.0; Media Cybernetics, Silver Spring, MD).

Sheep from the long-term cell tracking protocol were sacrificed after the final CMR scan (60 days post-AMI). All hearts were processed as outlined above and stained for macrophages with mouse anti-human CD68, Clone KP1 (Dako, Glostrup, Denmark), whereas the presence of intracellular iron was detected by Prussian blue staining. Microscopical analysis and quantification were done under ×40 magnifications through the whole surface of each section, and the scanned area was 162.5±24.0 mm^2 for BMMSC and 189.5±38.0 mm^2 for BMMSC-HIF. Sheep sacrificed at 7 days were used for short-term cell tracking and for immunohistochemistry. For short-term cell tracking analysis, hearts were fixed in 4% formaldehyde, cryoprotected in a 30% sucrose solution at 4°C until complete tissue penetration, and embedded in Cryoplast (Biopack, Buenos Aires, Argentina). BMMSCs labeled with CellTracker Red CMTPX Dye were detected by fluorescence microscopy in 7-μm-thick cryosections. For immunohistochemistry, hearts were treated as above for quantification of arteriolar and capillary densities. The scanned area was 135.7±31.7 mm^2 for the placebo group, 142.1±14.8 mm^2 for BMMSC, and 151.1±41.4 mm^2 for BMMSC-HIF. In addition, staining with phospho-histone-3 antibody (Ser10; Cell Signaling Technology) and mouse monoclonal antibody Ki67 antigen (Leica Biosystems,

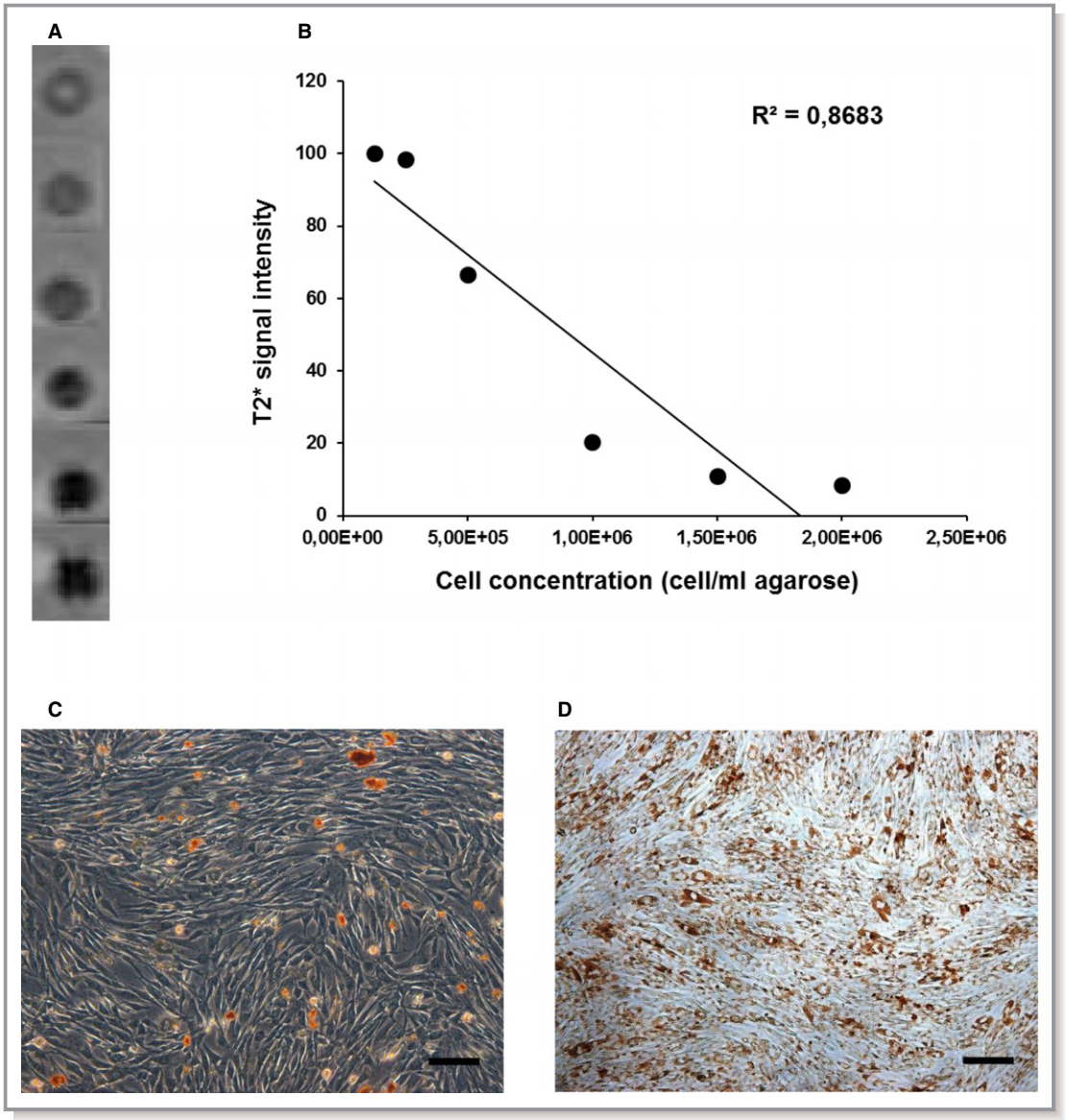

Figure 2. Magnetic resonance T2* images of tubes filled with agar containing an increasing number of magnetically labeled cells (A) and the calibration curve of T2* emitted intensity by each tube (B). Images of in vitro ovine bone marrow mesenchymal stromal cells 25% labeled prepared to injection (C) and 100% labeled (D) with 0.1 mg/mL of superparamagnetic iron oxide nanoparticles. Bars: 200 μm.

Newcastle, UK) to detect cardiomyocyte proliferation were used. It is important to notice that the immunohistochemistry studies at 7 days post-AMI included 4 sheep receiving placebo. Microscopical analysis and quantification were performed using hematoxylin and Mallory staining (without acid fuchsin to avoid nuclei staining), respectively, under ×100 magnifications on the whole surface of each section, and only the cells clearly defined as cardiomyocytes on the basis of their shape and presence of striations were considered. To detect apoptosis in paraffin sections of tissue from peri-infarct zones of placebo, BMMSC and BMMSC-HIF groups, the terminal deoxynucleotidyl transferase dUTP nick end labeling (TUNEL) assay was performed using the In situ cell death detection kit (Roche, Basel, Switzerland) detecting rhodamine-positive nuclei by fluorescence microscopy. Nuclei were double stained with 4',6-diamidino-2-phenylindole (DAPI), and the results are expressed as the percentage of TUNEL-positive nuclei of the total number of nuclei. The scanned area was 98.0±25.1 mm^2 for the placebo group, 94.4±10.3 mm^2 for BMMSC, and 85.6±34.9 mm^2 for BMMSC-HIF.

In Vivo Gene and Protein Expression

In all sheep belonging to the short-term protocol, myocardial tissue samples from the peri-infarct zone and a zone remote

to the infarct were taken and stored in liquid nitrogen at −80°C. RNA was extracted using the RNeasy minikit (Qiagen) and RT-qPCR was done to quantify gene expression of both mutated and wild-type HIF1-α and the downstream angiogenic factors erythropoietin (EPO), inducible nitrous oxide synthase (iNOS), vascular endothelial growth factor (VEGF), and angiopoietin-1 (ANGP-1), using the appropriate following primers: EPO (forward, 5′-ACGATGGGCTGTGCAGAAG-3′; reverse, 5′-CCTTGGTGTCTGGGACAGTGA-3′); iNOS (forward, 5′-GATGCAGAAGGCCATGTCATC-3′; reverse, 5′-CTCCCTGTCT CTGTTGCAAAGA-3′); VEGF (forward, 5′-GCCCACTGAGGAGTTC AACATC-3′; reverse, 5′-CTGGCTTTGGTGAGGTTTG-3′); ANGP-1 (forward, 5′-CAGAGCAGACCAGGAAGTT-3′; reverse, 5′-TCCAG CAGTTGTATTTCAAGTCG-3′). The primers for wild-type and mutated form of HIF1-α and GAPDH have been described above.

To detect the presence of angiogenic proteins, arrays spotted with human-specific antibodies (Proteome Profiler Human Angiogenesis Antibody Array; ARY007; R&D Systems, Minneapolis, MN) were performed according to the manufacturer's protocol in peri-infarct myocardial tissue lysates from each experimental group.

Statistical Analysis

Variables were analyzed with 1-way-ANOVA-Tukey for inter-group comparisons or 2-way-ANOVA-Bonferroni for inter- and intra-group comparisons, using GraphPad Prism software (version 5.0; GraphPad Software Inc., La Jolla, CA). Statistical significance was set at $P<0.05$ (2-tailed). Data are expressed as mean±SEM.

Results

Animal Surgical Outcome

Of a total of 44 operated sheep, 3 died of irreversible ventricular fibrillation before the intramyocardial injection procedure, and 3 (1 treated with BMMSC and 2 with placebo) died of unknown cause during follow-up. These 3 sheep were replaced with new animals. Consequently, results from 38 sheep are reported. Eighteen sheep were used for the main protocol, 8 for the long-term cell tracking protocol, and 12 for the short-term cell tracking and gene expression protocol. Note that 4 of these 12 sheep are placebo animals that did not undergo cell tracking.

BMMSCs Were Successfully Characterized and Transfected

Flow cytometry characterization revealed that the isolated BMMSCs were positive for CD44, and CD166, but negative for CD45 (Figure 3A). Likewise, BMMSCs were amenable to differentiation into adipogenic, chondrogenic, and osteogenic linages after 2 weeks of culture (Figure 3B). Transfection efficiency measured by GFP fluorescence was higher ($P<0.001$) for the minicircle vector compared to conventional plasmids at day 1 (39.7±0.7% vs 23.2±2.4%), day 3 (70.1±2.4% vs 36.5±3.2%), and day 6 (79.3±0.4% vs 25.6±2.9%) post-transfection (Figure 3C). Moreover, whereas transfection efficiency with MC showed a temporal increase, it decayed ($P<0.05$) with the conventional plasmid at day 6 compared to day 3 (Figure 3C). In BMMSC-HIF, HIF1-α mRNA increased 3×10^6-fold from days 1 to 6, and mRNA expression of wild-type of HIF1-α was almost undetectable in the BMMSC and BMMSC-HIF (Figure 3D). The increase in HIF1-α mRNA expression was further supported by immunoblotting for HIF1-α protein levels, which demonstrated a significant increase in BMMSC-HIF compared to controls (Figure 3E and 3F).

Cell Retention Is Enhanced by HIF1-α-Transfected BMMSCs

To investigate whether HIF1-α overexpression improves cell retention, BMMSCs were labeled with fluorescent CMTPX dye (short-term tracking) or with SPIO detectable as hypointense zones in T2* CMR sequences (mid- and long-term tracking). At 7 days, BMMSC and BMMSC-HIF were readily visible in injected areas (Figure 4A). For long-term tracking, CMR in animals injected with SPIO-labeled BMMSC-HIF and BMMSC were performed at 1, 30, and 60 days postinjection. CMR showed retention of injected cells over time. Group analysis showed that, as expected, the initial volume of hypointense zones was similar for both groups at day 1 (BMMSC: 1.55±0.07 mL; BMMSC-HIF: 1.58±0.1 mL; P=NS [not significant]), and the hypointense volume decreased significantly at 30 and 60 days, compared to day 1 ($P<0.001$), but BMMSC-HIF presented significantly higher ($P<0.001$) T2* hypointense signal than the BMMSC group at 30 days (1.3±0.12 vs 0.59±0.06 mL, respectively) and at 60 days (1.15±0.11 vs 0.51±0.03 mL, respectively). Estimation of the number of retained cells in peri-infarct zones showed that BMMSC and BMMSC-HIF had similar number of cells at day 1 (9 193 326±995 774 [45.9%] vs 9 774 688±859 426 [48.8%], respectively; P=NS). Sheep receiving BMMSC-HIF presented a higher number of retained cells than BMMSC at day 30 (6 296 250±965 348 vs 3 076 365±127 537; $P<0.001$) and day 60 (5 855 108±1 126 621 vs 2 808 179±89 615; $P<0.001$), indicating that 14.04% of injected cells in the BMMSC group and 29.27% in the BMMSC-HIF group were retained at the end of follow-up (Figure 4B through 4D).

To evaluate whether the detected iron corresponded to BMMSCs effectively retained in the myocardium or to iron particles phagocytized by macrophages, 2 consecutive

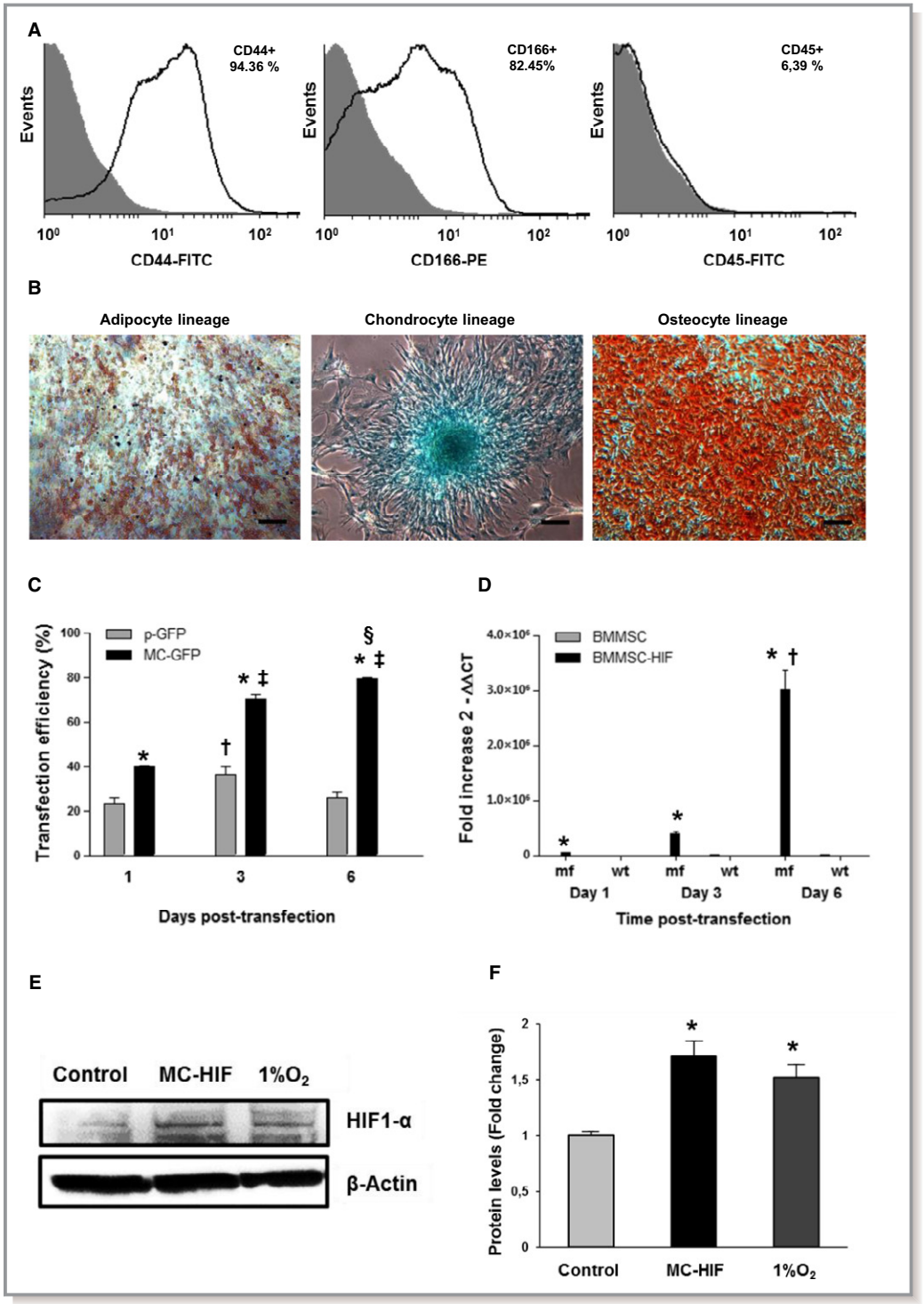

Figure 3. Ovine bone marrow mesenchymal stromal cells (BMMSC) characterization and transfection efficiency. A, BMMSCs were $CD44^{+}$, $CD166^{+}$, and CD45−. B, Differentiation of BMMSC into adipocytes (left), chondrocytes (mid), and osteocytes (right). Bars: 200 μm. C, Transfection efficiency (TE) at 1, 3, and 6 days post-transfection of the minicircle-GFP (MC-GFP) as compared with conventional plasmid-GFP (p-GFP). *P<0.001 vs p-GFP; $^{\dagger}P$<0.01 vs day 1 and day 6; $^{\ddagger}P$<0.01 vs day 1 and day 3; $^{\S}P$<0.05 vs day 3. D, Expression of mutant form (mf) and wild-type form (wt) of HIF1-α (RT-qPCR) at 1, 3, and 6 days post-transfection. *P<0.001 vs BMMSC; $^{\dagger}P$<0.001 vs day 1 and day 3. E, Representative immunoblot of HIF1-α in BMMSC, BMMSC-HIF, and BMMSC exposed to hypoxia for 24 hours. F, Densitometry analysis of (E) (*P<0.05). GFP indicates green fluorescent protein; HIF, hypoxia-inducible factor; RT-qPCR, reverse-transcriptase quantitative polymerase chain reaction.

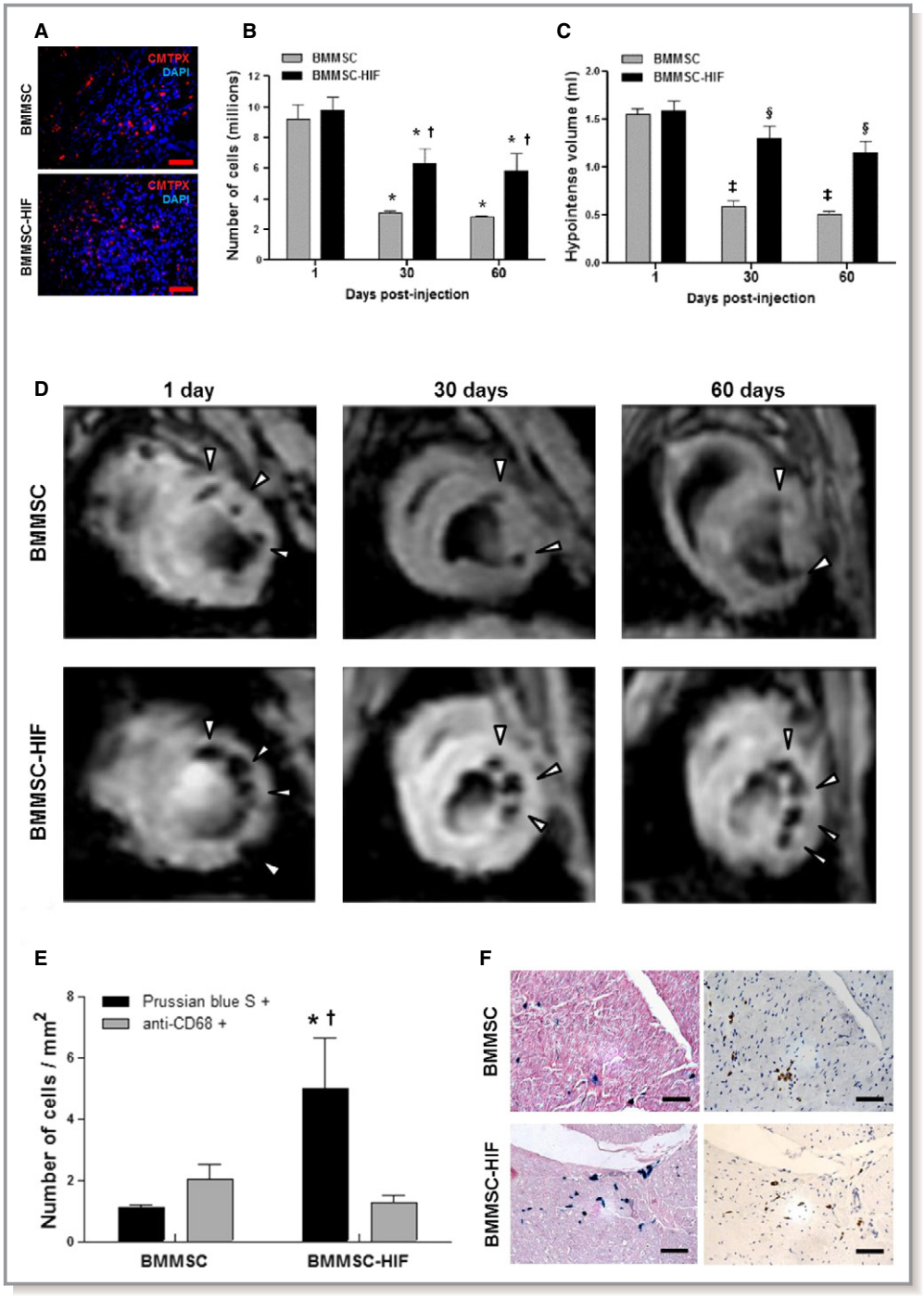

Figure 4. Cell retention. A, Short-term (7 days) tracking: injected cells stained with Red CMTPX dye are readily visible in nontransfected bone marrow mesenchymal stromal cells (BMMSC; upper) and HIF1-α-transfected bone marrow mesenchymal stromal cells (BMMSC-HIF; lower) groups (bars: 50 μm). B and C, Long-term cell retention: In the BMMSC-HIF group (n=4), the number of cells and hypointense volume remains higher than in the BMMSC group (n=4) over time. **P*<0.001 vs day 1; †*P*<0.05 vs BMMSC; ‡*P*<0.001 vs day 1; §*P*<0.001 vs day 1 and vs BMMSC. D, Long-term tracking: BMMSC marked with superparamagnetic oxide iron nanoparticles are visible (arrowheads) at 1, 30, and 60 days postinjection. E, Histological staining with Prussian blue and anti-CD68 antibody. BMMSC group (n=4) and BMMSC-HIF group (n=4). **P*<0.05 vs BMMSC; †*P*<0.05 vs anti-CD68. F, Representative Prussian-blue–stained slices (left) and anti-CD68-stained slices (right) of an animal of BMMSC (upper) and BMMSC-HIF (lower) groups. DAPI indicates 4',6-diamidino-2-phenylindole; HIF, hypoxia-inducible factor.

paraffin-embedded tissue sections 4 μm in thickness were stained; one with Prussian blue and the other with an antibody against CD68. Whereas the number of CD68-positive cells was similar for BMMSC (2.02±0.51 cells/mm^2) and BMMSC-HIF (1.27±0.23 cells/mm^2; *P*=NS), Prussian blue–positive cells were more abundant in the samples from BMMSC-HIF (5.0±1.67 cells/mm^2 vs 1.08±0.09 cells/mm^2; *P*<0.05; Figure 4E), suggesting that, in BMMSC-HIF, a significant part of the detected iron effectively corresponded to the injected cells (Figure 4F).

BMMSC-HIF Induced the Largest Reduction in Infarct Size

Infarct size, calculated from CMR and expressed in milliliters of infarcted tissue, is depicted in Figure 5A. The initial ischemic region after 1 day post-AMI was similar in all groups (placebo: 9.1±0.2 mL; BMMSC: 9.4±0.4 mL; BMMSC-HIF: 9.6±0.3 mL; *P*=NS). Compared to placebo, infarct size was smaller by 18.8% for BMMSC and 49.6% for BMMSC-HIF at 30 days post-treatment, and 36.3% and 66.6%, respectively, at end of follow-up. At both 30 and 60 days, the absolute values for infarct size in BMMSC and BMMSC-HIF were significantly lower than placebo. Paired comparisons showed that the scar-size reduction from the initial ischemic region at day 1 to 60 days scar size was 44.1±4.7% for the BMMSC group and 71.7±1.3% for BMMSC-HIF. By contrast, the placebo group did not show significant reductions between the initial ischemic damage at day 1 and final scar size at day 60 postinjection. Examples of LV short-axis CMR images are shown in Figure 5B, and examples of LV endocardial aspect of infarct size are depicted in Figure 5C.

BMMSC-HIF Improved Cardiac Function

EDV did not differ among groups at day 1 (placebo: 63.2±2.6 mL; BMMSC: 62.1±3.1 mL; BMMSC-HIF: 63.06±1.9 mL; *P*=NS). The placebo group exhibited increased EDV at day 30 (70.5±2.5 mL) and day 60 (74.5±1.0 mL) compared to day 1 (*P*<0.05 and <0.01, respectively). In BMMSC and BMMSC-HIF groups, EDV did not change over time (*P*=NS; Figure 6A). ESV was similar among groups at day 1 (placebo: 46.7±2.4 mL; BMMSC: 45.2±2.2 mL; BMMSC-HIF: 45.7±1.4 mL; *P*=NS). In the BMMSC group, ESV was lower than in the placebo group at end of follow-up (BMMSC: 42.9±1.1; placebo: 52.1±2.1 mL; *P*<0.01). In the BMMSC-HIF group, ESV decreased at day 30 (38.2±0.9 mL) and further at day 60 (29.0±1.7 mL) compared to its baseline value (*P*<0.01 and <0.001, respectively). In addition, it was lower than placebo at 30 days (*P*<0.001) and also lower (*P*<0.001) than placebo and BMMSC at 60 days (Figure 6B). As a result of the relative changes in EDV and ESV, %EF increased from

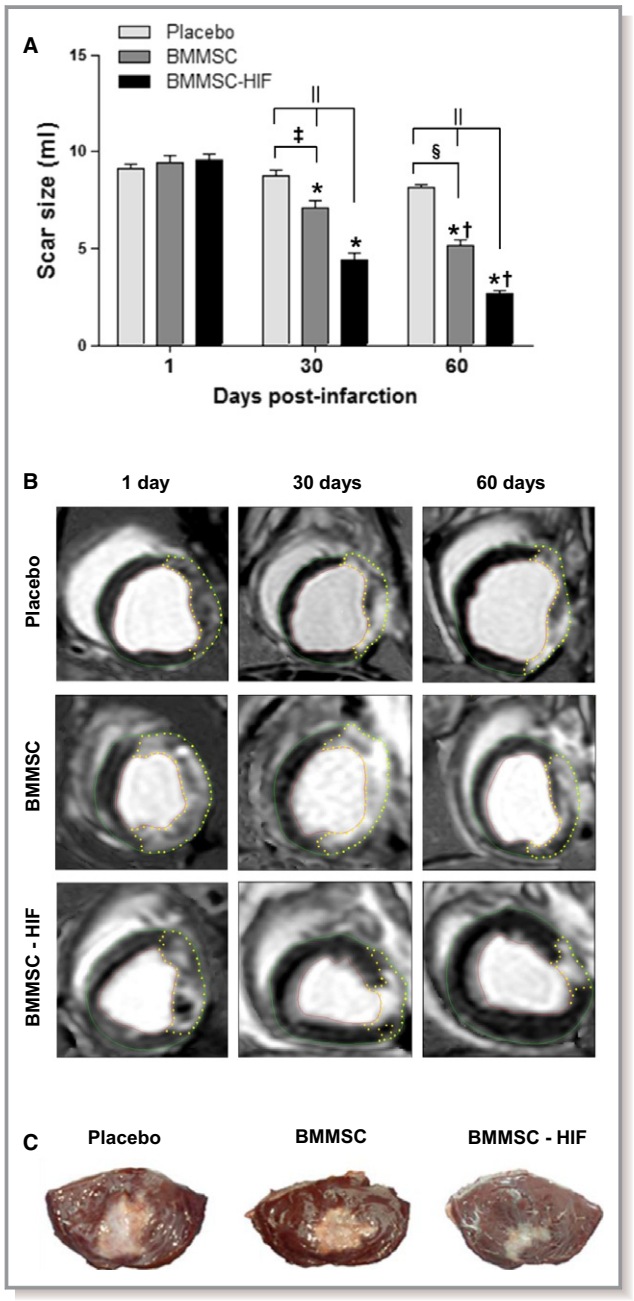

Figure 5. A, Ischemic region and infarct size assessed from cardiac magnetic resonance (CMR). Extent of scar size decrease is significantly larger in the group treated with HIF1-α transfected bone marrow mesenchymal stromal cells (BMMSC-HIF) at 30 and 60 days postinfarction. Placebo group (n=6), BMMSC group (n=6), and BMMSC-HIF group (n=6). *P<0.001 vs day 1; †P<0.001 vs day 30; ‡P<0.01 vs placebo; §P<0.001 vs placebo; ‖P<0.001 vs placebo and BMMSC groups. B, Representative short-axis LV images (late gadolinium enhancement) at end diastole at 1, 30, and 60 days post-treatment. The animal from the BMMSC-HIF group displays the maximum scar-size reduction. Infarct borders are dotted in yellow; red line indicates endocardium and green line indicates epicardium. C, Endocardial aspect of representative hearts from each group opened along the posterior interventricular sulcus. The pale zone corresponds to the infarct scar. HIF indicates hypoxia-inducible factor; LV, left ventricle.

27.1±1.3% at day 1 to 36.7±1.1% at day 30 and to 37.8±1.0% at day 60 (both $P<0.001$) in the BMMSC group, and from 27.2±2.6% at day 1 to 42.4±0.9% at day 30 and further to 53.3±2.0% at day 60 (both $P<0.001$) in the BMMSC-HIF group. Both groups displayed significant differences compared to placebo ($P<0.05$ and <0.01, respectively) at both time points. However, at the end of follow-up, %EF was highest in BMMSC-HIF and significantly different ($P<0.001$) not only from placebo, but also from BMMSC (Figure 6C). Video recordings of CMR scans at 1 and 60 days post-treatment showed that BMMSC-HIF induced a noticeable recovery of wall motion in the infarcted zone, whereas in the placebo-treated animals, the infarcted wall remained akinetic. Selected illustrative images taken from videos of an animal of each group are shown in Figure 6D. Additionally, CMR movies of a placebo-treated (Videos S1 and S2) and a BMMSC-HIF-treated animal (Videos S3 and S4) are provided.

As a measurement of interstitial fibrosis in normoperfused zones remote to AMI, Picrosirius red–stained areas were significantly higher ($P<0.001$) in the placebo group (8.46±0.62%) than BMMSC (4.71±1.16%) and BMMSC-HIF (2.78±0.27%; $P<0.001$ vs BMMSC), indicating that the placebo group underwent significant remodeling over 2 months postinfarction, which was prevented by both BMMSC and BMMSC-HIF treatments (Figure 6E and 6F).

BMMSC-HIF Promoted Microvascular Proliferation

Microvascular densities were assessed in sheep sacrificed at 7 and 60 days post-treatment. Compared to placebo and BMMSC, arteriolar and capillary densities were significantly increased in BMMSC-HIF at indicated time points ($P<0.001$; Figure 7A and 7B). The arterioles of animals from the BMMSC-HIF group presented higher CSD and WTh at 7 and 60 days post-treatment ($P<0.001$) without significant changes in LD. Both WTh and CSD were higher at day 60 compared to day 7 ($P<0.001$). In the BMMSC group, the arterioles exhibited higher WTh at day 7 compared to placebo ($P<0.05$), without significant changes at day 60 post-treatment. In the placebo group, arteriolar diameters and WTh remained stable over time (P=NS). Representative histological images are shown in Figure 7C, and the absolute values are listed in Tables 1 and 2. In remote zones, there were no significant differences for capillary or arteriolar densities at any time points (data not shown).

BMMSC-HIF Reduced Apoptosis in the Heart and Induced Cell Proliferation

To measure apoptosis in the peri-infarct, TUNEL assay was performed at 7 days post-treatment (Figure 8A). Apoptosis was 53.37±4.2% in placebo, 35.32±1.64% in BMMSC ($P<0.01$ versus placebo), and 19.6±0.37% ($P<0.001$) in BMMSC-HIF.

On the other hand, the percent cardiomyocyte nuclei positive for the mitotic marker, pH3, was highest in BMMSC-HIF (50.08±5.13%/mm^2), followed by BMMSC (34.63±2.69%/mm^2) and placebo (15.74±1.41%/mm^2; $P<0.001$ vs BMMSC-HIF and $P<0.05$ vs BMMSC; Figure 8B).

In addition, the presence of Ki67-positive cardiomyocytes nuclei were also increased in BMMSC-HIF (placebo: 0.22±0.03 cells/mm^2; BMMSC: 0.25±0.07 cells/mm^2; BMMSC-HIF: 0.5±0.05 cells/mm^2, $P<0.05$ vs placebo and BMMSC; Figure 9A and 9B). Some of the Ki67-positive nuclei showed ongoing mitosis (Figure 9C).

HIF1-α Transfection Enhanced the Expression of HIF1 Downstream Genes

Mutated HIF1-α mRNA expression was significantly higher in the peri-infarct area of animals treated with BMMSC-HIF and was undetectable in the remote normoperfused zones, as well as in sheep from BMMSC and placebo. mRNA of wild-type HIF1-α was barely detectable in the peri-infarct zones and in the remote myocardium of all groups. HIF1 downstream genes involved in angiogenesis and tissue repair (EPO, iNOS, VEGF, and ANGP-1) were also significantly upregulated in the peri-infarct of animals treated with BMMSC-HIF ($P<0.01$). Whereas EPO and iNOS were detectable only in BMMSC-HIF, VEGF and ANGP-1 were also upregulated in BMMSC-treated animals, albeit at a lower level compared to BMMSC-HIF. Expression levels of HIF1-α and the aforementioned genes in peri-infarct and remote zones are shown in Figure 10.

Discussion

Our results showed that intramyocardial delivery of allogeneic BMMSCs overexpressing a mutant, oxygen-resistant form of HIF1-α reduced infarct size and improved LV function to a larger extent than BMMSCs in sheep with AMI at 2 months post-treatment, which was associated with increased neovascularization and reduced apoptosis in the heart along with increased expression of proangiogenic genes. In animal models of AMI, intramyocardial implant of unmodified BMMSCs has been shown to induce variable infarct-size reductions. In some studies, reductions of over 50% have been reported.[18,19] In our BMMSC-treated animals, at 2 months post-treatment, infarcts were 36% smaller than in sheep receiving placebo, and 44% smaller with regard to their initial size. However, the extent of scar-size limitation was significantly larger for animals receiving BMMSC-HIF (66% compared to placebo at 60 days and 71% compared to initial postinfarct size). Given that the infarct-limiting effect

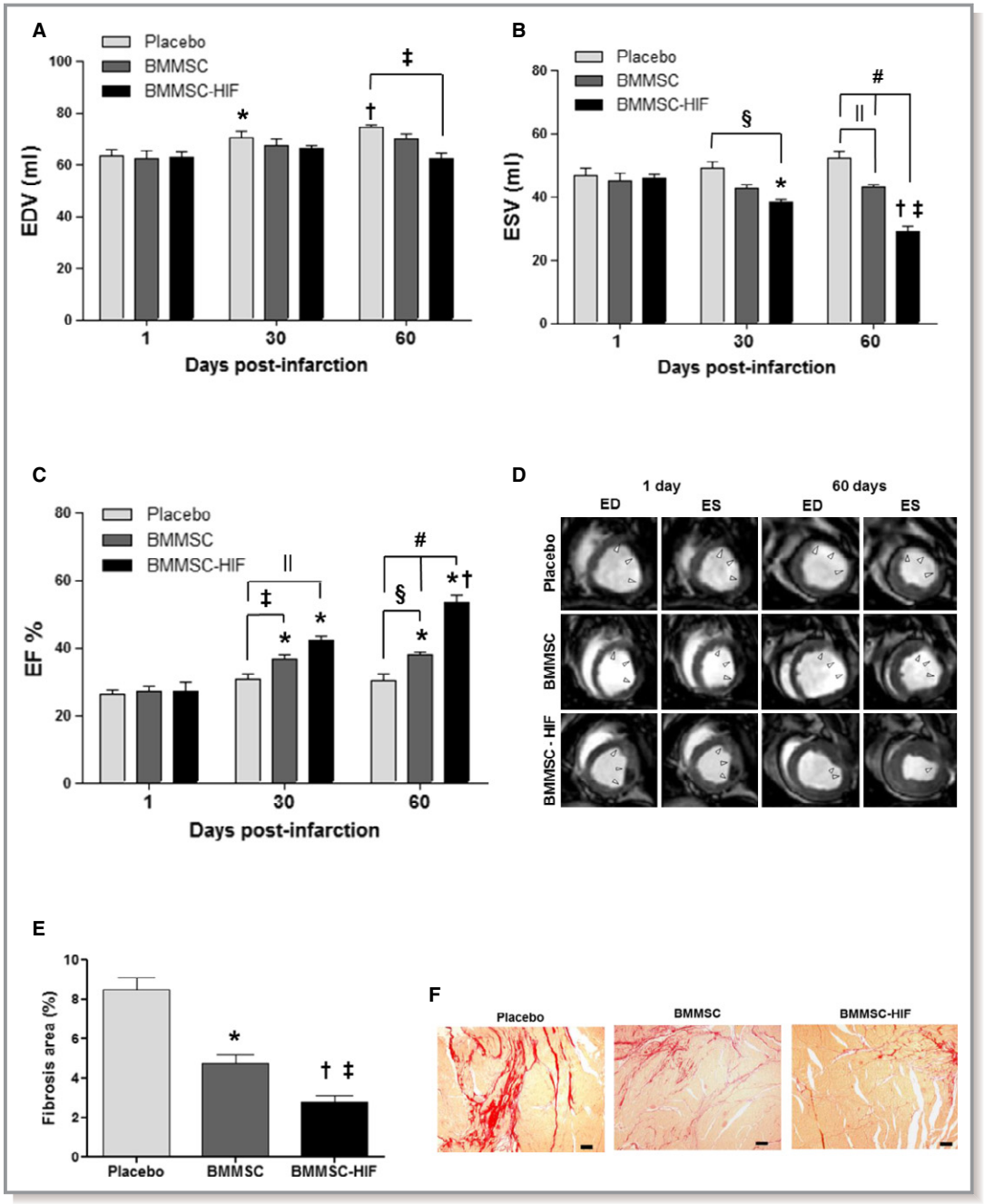

Figure 6. Left ventricular function. A, End diastolic volume (EDV); **P*<0.05 vs day 1; †*P*<0.01 vs day 1; ‡*P*<0.001 vs placebo. B, End systolic volume (ESV): **P*<0.01 vs day 1; †*P*<0.001 vs day 1; ‡*P*<0.01 vs day 30; §*P*<0.001 vs placebo; ‖*P*<0.01 vs placebo; #*P*<0.001 vs placebo and BMMSC. C, Ejection fraction (%EF): **P*<0.001 vs day 1; †*P*<0.001 vs day 30; ‡*P*<0.05 vs placebo; §*P*<0.001 vs placebo; ‖*P*<0.001 vs placebo; #*P*<0.001 vs placebo and BMMSC. D, Left ventricular function as assessed by cardiac magnetic resonance (CMR). Representative short-axis images at 1 and 60 days postinfarction taken from video recordings by a placebo, a BMMSC, and BMMSC-HIF animal. At day 1, the akinetic zone (arrowheads) was similar among groups. At day 60, the zone showing akinesia on day 1 displayed systolic thickening in the BMMSC-HIF-treated animal. Note that precise infarct limits are not seen because video recordings are taken before late gadolinium enhancement. For complete short- and long-axis video recordings, please see Videos S1 through S4. BMMSC: group receiving nontransfected bone marrow mesenchymal stromal cells; BMMSC-HIF: group receiving HIF1-α-transfected bone marrow mesenchymal stromal cells. E, Interstitial fibrosis. Fibrosis area (%) is higher in placebo group than BMMSC and BMMSC-HIF at 60 days post-treatment (**P*<0.01 vs placebo; †*P*<0.01 vs BMMSC; ‡*P*<0.001 vs placebo). F, Placebo group (n=6), BMMSC group (n=6), and BMMSC-HIF group (n=6). ED indicates end diastolic; ES, end systolic; HIF, hypoxia-inducible factor.

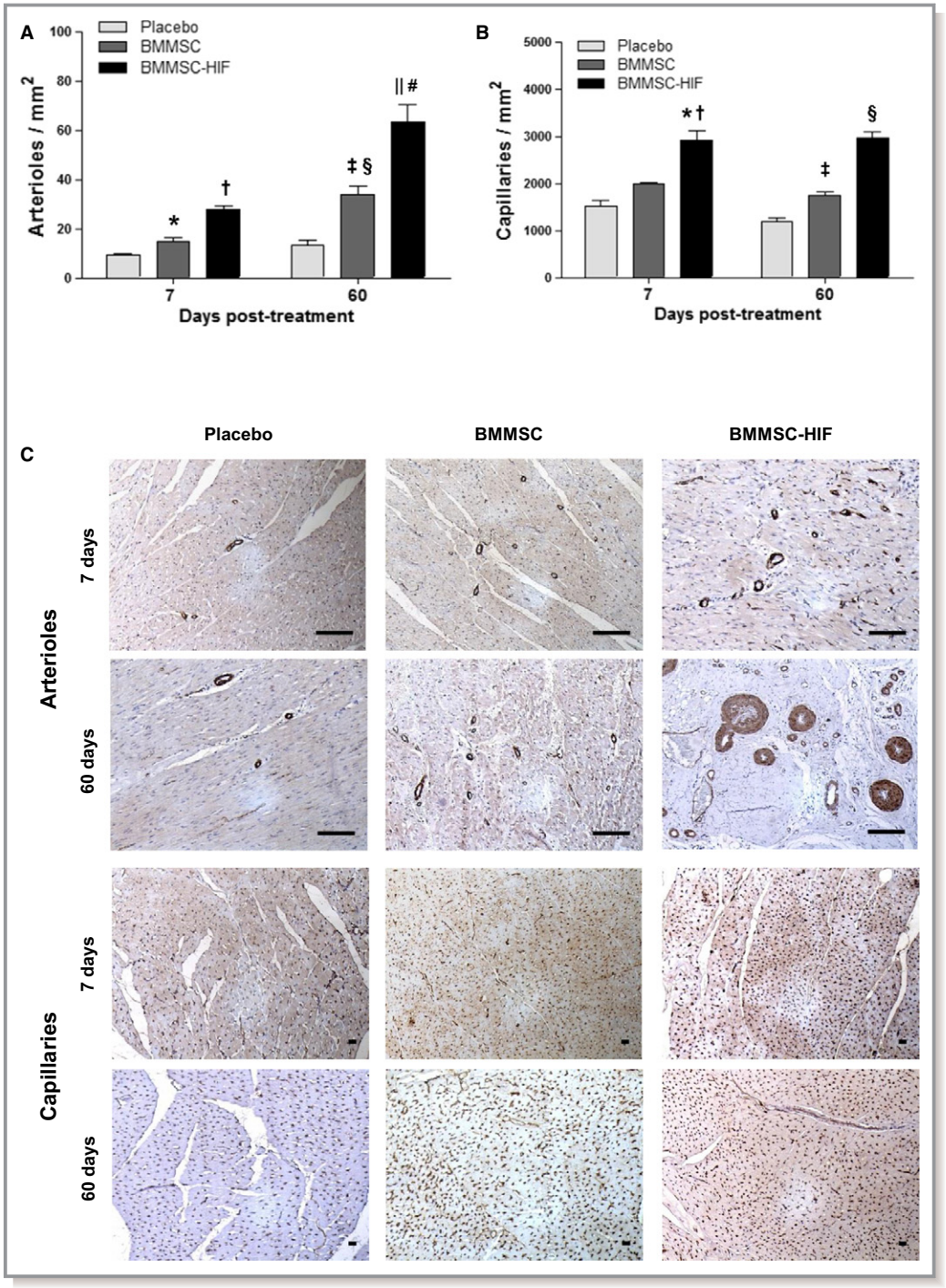

Figure 7. Microvascular density. A, Arteriolar density is highest in BMMSC and BMMSC-HIF at 7 and 60 days post-treatment (*P<0.05 vs placebo; †P<0.001 vs placebo and BMMSC; ‡P<0.01 vs placebo; §P<0.05 vs day 7; ‖P<0.001 vs placebo and vs day 7; #P<0.01 vs BMMSC). B, Capillary density is higher at 7 and 60 days in BMMSC and BMMSC-HIF (*P<0.01 vs BMMSCs; †P<0.001 vs placebo; ‡P<0.01 vs placebo; §P<0.001 vs placebo and BMMSC). C, Representative histological images from an animal of each group at 7 and 60 days showing arterioles (smooth-muscle actin antibody/hematoxilin; bars: 100 μm) and capillaries (Biotinylated Euonymous Europaeus Lectin antibody/hematoxilin; bars: 20 μm). BMMSC: group receiving nontransfected bone marrow mesenchymal stromal cells; BMMSC-HIF: group receiving HIF1-α-transfected bone marrow mesenchymal stromal cells. Note higher arteriolar wall thickness in the BMMSC-HIF group at 60 days. Microvacular density at 7 days: placebo group (n=4), BMMSC group (n=4), and BMMSC-HIF group (n=4). Microvascular density at 60 days: placebo group (n=6), BMMSC group (n=6), and BMMSC-HIF group (n=6). HIF indicates hypoxia-inducible factor.

Table 1. Arteriolar and Capillary Density at 7 and 60 Days Post-Treatment in Peri-Infarct Zone

	Arterioles/mm^2		Capillaries/mm^2	
	Day 7	Day 60	Day 7	Day 60
Placebo	9.1±0.8	13.4±1.8	1521±129	1200±59
BMMSC	15.0±1.4*	33.6±3.8‡§	1984±39	1743±64‡
BMMSC-HIF	27.8±1.5†	63.2±6.9$^{‖#}$	2905±210*†	2967±129§

Day 7: n=4/group; day 60: n=6/group. BMMSC indicates group treated with nontransfected bone marrow mesenchymal stromal cells; BMMSC-HIF, group treated with HIF1-α-transfected bone marrow mesenchymal stromal cells. HIF, hypoxia-inducible factor.
Arteriolar density: *P<0.05 vs placebo; $^{†}P$<0.001 vs placebo and BMMSC; $^{‡}P$<0.01 vs placebo; $^{§}P$<0.05 vs day 7; $^{‖}P$<0.001 vs placebo and vs day 7; $^{\#}P$<0.01 vs BMMSC.
Capillary density: *P<0.01 vs BMMSC; $^{†}P$<0.001 vs placebo; $^{‡}P$<0.01 vs placebo; $^{§}P$<0.001 vs placebo and BMMSC.

progressed over time, it is plausible to assume that enhanced long-term cell retention permitted a persistent effect of overexpressed factors on neovascularization and reduction of apoptosis in the whole heart.

Importantly, CMR allowed comparisons to be performed on a paired basis. This was particularly advantageous, because sheep as a species display heterogeneous LAD artery distribution, with interindividual variations that make it difficult to achieve similar infarct sizes across the experimental population.[20] The use of CMR at 3 time points allowed us not only to compare infarct size against the initial ischemic damage extension, but also to observe how it evolved over time.

Given that there were no changes in scar size, which was accompanied with increased EDV over time in placebo group, LV remodeling occurred in placebo-treated animals. This remodeling was prevented by injection of both BMMSC and BMMSC-HIF. Treatment with BMMSC improved LV function at 1 month and prevented EF from deteriorating later on. However, the largest improvement in LV function was achieved in BMMSC-HIF. Given that this improvement arose from a significant 37% decrease in ESV with unchanged EDV, it is reasonable to assume that the angiogenic and improved cardiac cell proliferation effects of BMMSC-HIF resulted in increased LV contractile performance. Indeed, an evident recovery of wall motion and systolic thickening of the ischemic LV wall at the end of follow-up was observed in video recordings of CMR scans of these animals (see Videos).

In terms of neovascularization, both BMMSC and BMMSC-HIF increased arteriolar density at 7 and 60 days post-treatment, with a significantly larger degree in the latter. Given that BMMSCs secrete a number of paracrine molecules involved in migration and proliferation of vascular smooth-muscle cells, enhanced arteriolar growth in animals receiving BMMSC was expected.[21–24] The fact that this effect was stronger in BMMSC-HIF treated sheep can be attributed to HIF-mediated overexpression of angiogenic genes as well as enhanced cell retention, as indicated by our long-term tracking experiments. Capillary density was also maximal in BMMSC-HIF at both time points. Interestingly, whereas arterioles continued to proliferate between day 7 and day 60 in both BMMSC and BMMSC-HIF, capillaries did not proliferate similarly, and their density remained almost unchanged with regard to its value at 7 days. This may be attributed to the fact that ANGP-1, principally involved in arteriogenesis, displayed larger overexpression than VEGF, a classic mitogen of endothelial cells. In our study, overexpression of ANGP-1 may have contributed to the arteriolar wall hypertrophy in the BMMSC-HIF group at the end of follow-up.

Of note, the increase of pH3-positive cardiomyocyte nuclei observed in the peri-infarct zone in BMMSC-HIF in sheep sacrificed at 7 days post-treatment may suggest that HIF1-α downstream genes induce reentry of adult cardiomyocytes into mitosis, which may contribute to the cardioprotective effects of BMMSCs. This observation is consistent with previous studies in rats with AMI reporting HIF1-α-induced reentry of adult cardiomyocytes into the cell cycle using mesenchymal stem cells (MSCs) previously transduced with adenovirus-HIF1-α[25] or after direct transduction with adenovirus-HIF1-α.[26] In a recent study, a highly significant correlation was demonstrated between the proliferative

Table 2. Cross-Sectional Diameter, Wall Thickeness, and Lumen Diameter of Arterioles at 7 and 60 Days Post-Treatment in Peri-Infarct Zone

	Day 7			Day 60		
	Placebo	BMMSC	BMMSC-HIF	Placebo	BMMSC	BMMSC-HIF
CSD, μm	17.08±0.69	21.0±0.97	27.82±1.54*	18.09±1.77	24.06±1.6	46.11±2.27*†
LD, μm	6.57±0.47	6.59±0.45	6.98±0.4	7.76±0.35	7.96±0.38	7.96±0.47
WTh, μm	5.25±0.35	7.2±0.28*	10.42±0.75†	5.17±0.88	8.05±0.82	19.07±1.26†‡

Day 7: n=4/group; day 60: n=6/group. BMMSC: group treated with nontransfected bone marrow mesenchymal stromal cells; BMMSC-HIF: group treated with HIF1-α-transfected bone marrow mesenchymal stromal cells. HIF indicates hypoxia-inducible factor.
Cross-sectional diameter (CSD): *P<0.001 vs placebo and BMMSC; $^{†}P$<0.001 vs 7 days. Lumen diameter (LD): no significant difference. Wall thickeness (WTh): *P<0.05 vs placebo; $^{†}P$<0.001 vs placebo and BMMSC; $^{‡}P$<0.001 vs 7 days.

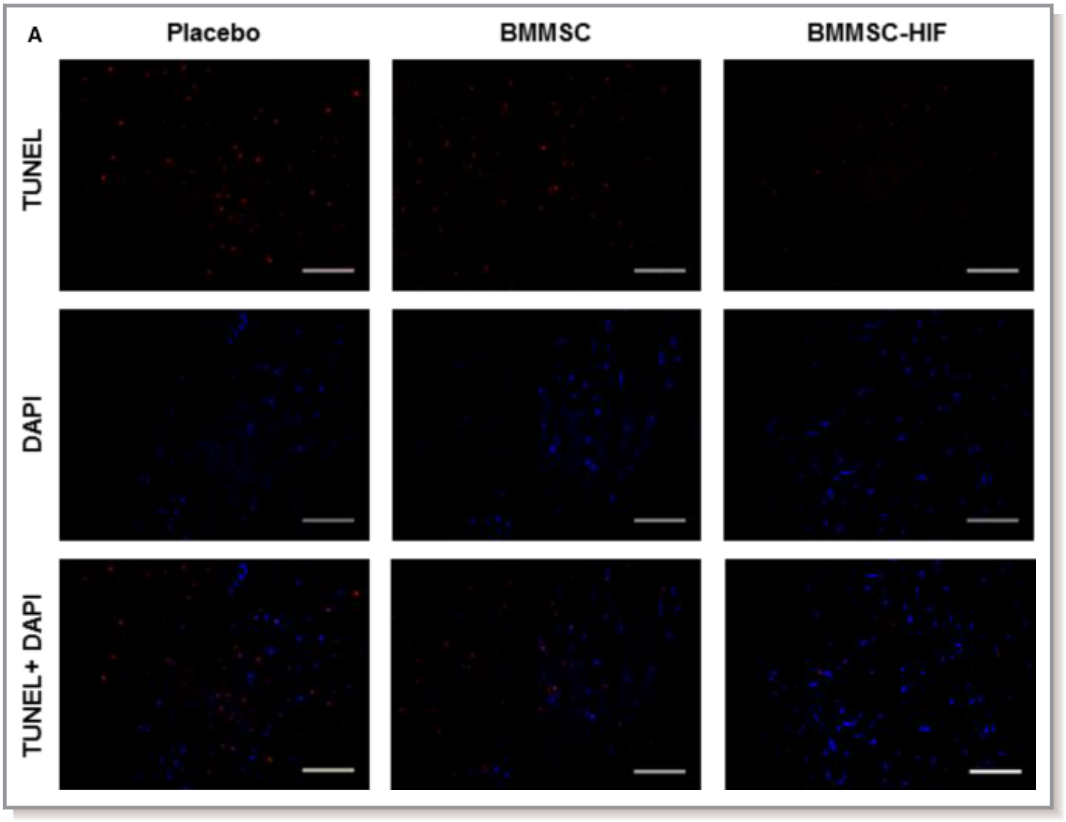

Figure 8. Heart apoptosis and mitotic cardiomyocytes. A, TUNEL assay. Examples of TUNEL-stained cardiac tissue from placebo (n=4), BMMSC (n=4), and BMMSC-HIF (n=4) groups. Percentage of apoptotic nuclei (red) were determined in relation of total number of DAPI-stained nuclei (light blue). Bars: 50 μm. Overall results of this assay are shown in (C): **P*<0.01 vs placebo; †*P*<0.001 vs placebo and BMMSC. B, Representative images of phospho-histone-3–positive (pH3+) nuclei (light brown colored nuclei) in peri-AMI tissue from BMMSC-HIF (n=4), BMMSC (n=4), and placebo (n=4) animals. Bars: 50 μm. Results are shown in (D): **P*<0.05 vs placebo; †*P*<0.001 vs placebo and BMMSC. BMMSC: group receiving nontransfected bone marrow mesenchymal stromal cells; BMMSC-HIF: group receiving HIF1-α-transfected bone marrow mesenchymal stromal cells. AMI indicates acute myocardial infarction; DAPI, 4',6-diamidino-2-phenylindole; HIF, hypoxia-inducible factor; TUNEL, terminal deoxynucleotidyl transferase dUTP nick end labeling.

cardiomyocytes and overexpression of HIF1-α downstream genes in the peri-infarct myocardium in primates.[27] VEGF, one of the HIF1 downstream genes, has been shown to induce adult cardiomyocyte mitosis in large mammalian models of ischemic heart disease.[28–30] It is therefore possible that overexpression of VEGF in our BMMSC-HIF-treated sheep promoted cardiomyocyte proliferation.

In stem cell–based cardiac regeneration, myocardial cell retention remains a challenge.[31] Among other factors, the cell delivery technique plays a key role. We treated our sheep using direct intramyocardial injections, a route shown to yield significantly higher cell retention than intracoronary and retrograde coronary venous routes.[32,33] However, even when using the intramyocardial route, it has been reported that within a few hours, cell retention dropped below 12%.[32] We also observed that VEGF-transfected BMMSCs injected into the peri-infarct of ovine myocardium, while abundant at 7 days, were very scarce 1 month after delivery.[24] In this study, we demonstrate a higher percentage of retained postinjection cells at day 1, which may be explained by the implementation of injection technique and also by the immunomodulatory characteristic of the BMMSCs, which may reduce the immune response preventing cell death.

In the present study, short-term tracking showed that BMMSC-HIF and BMMSC were readily visible, confirming our previous results. Regarding long-term retention, in agreement with past results,[34] we found that it decayed significantly at days 30 and 60, compared to day 1, in hearts receiving BMMSC and in BMMSC-HIF, but the percentage of retained BMMSC-HIF remained higher than BMMSC, which could be explained by overexpression of prosurvival genes, such as ANGP-1 and EPO. Prussian blue staining confirmed that iron-bearing cells were more abundant in BMMSC-HIF-treated hearts. To assess whether the enhanced CMR signals arose

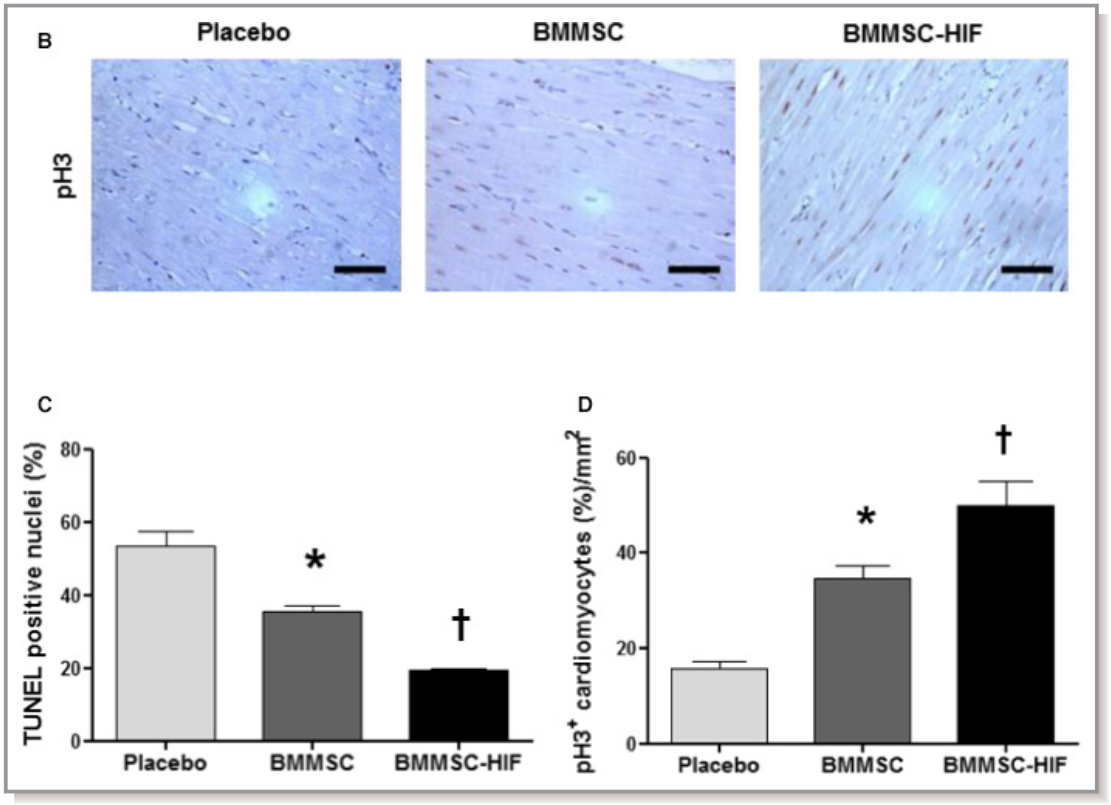

Figure 8. Continued.

from cardiac macrophages that engulfed the SPIO nanoparticles,[35] we quantified CD68-positive cells and found that in samples of BMMSC-HIF animals, Prussian blue–positive cells exceeded the amount of macrophages by more than 3-fold. This was not the case for sheep treated with BMMSC, which showed no significant differences between Prussian blue–positive and CD68-positive BMMSCs. Although not conclusive, these observations suggest that a large proportion of the hypointense CMR signal arose from BMMSC-HIF retained in the injected myocardium. Our results are in agreement with those from Drey et al.,[36] showing that in mice hearts injected with SPIO-BMMSCs labeled with a vital stain, the hypointense zones observed over 4 weeks corresponded to colocalization of both stains, confirming the retention of SPIO within vital BMMSCs.[36] The enhanced cell retention observed in our BMMSC-HIF-treated sheep may be attributed to HIF-mediated overexpression of cell prosurvival genes.[25,37] In fact, iNOS, a key cardioprotective gene in acute and chronic heart disease,[38] displayed a several-fold increased expression. In rats with AMI, Azarnoush et al. showed that survival and engraftment of intramyocardially delivered skeletal myoblasts were dramatically increased when myoblasts were coinjected with HIF1-α.[39] Moreover, it has been recently shown that overexpression of HIF1-α in human BMMSCs protects against cell death and apoptosis triggered by hypoxic and oxidative stress conditions.[40]

Because we did not perform a dose-response curve, we cannot state whether a higher amount of injected cells would have resulted in larger cardioprotection. In ovine AMI, Hamamoto et al. injected 25, 75, 225, and 450×10^6 MSCs in the peri-infarct and observed that the lower doses yielded the largest beneficial effects on infarct size and LV function.[41] The amount of cells we injected (20×10^6) was close to the lowest dose used by Hamamoto et al., and still effective, in that even without HIF1-α transfection, significant cardioprotection was achieved. Furthermore, in a recent study of intracoronary MSCs in sheep with AMI, Houtgraaf et al. showed that at 2 months post-treatment, similar effects on infarct size, microvascular growth, cardiomyocyte proliferation, and LV systolic and diastolic function were achieved with doses lower (12.5×10^6), comparable (25×10^6), and higher (50×10^6) than ours.[42] Taken together, these data suggest that larger amounts of injected cells would not have changed our results significantly.

Study Limitations

Although the sheep model is increasingly used in cardiovascular translational research, commercially available antibodies against sheep antigens are scarce, which limits precise characterization of diverse cells. We confined our cell-surface–based identification of BMMSCs to 3 antibodies.

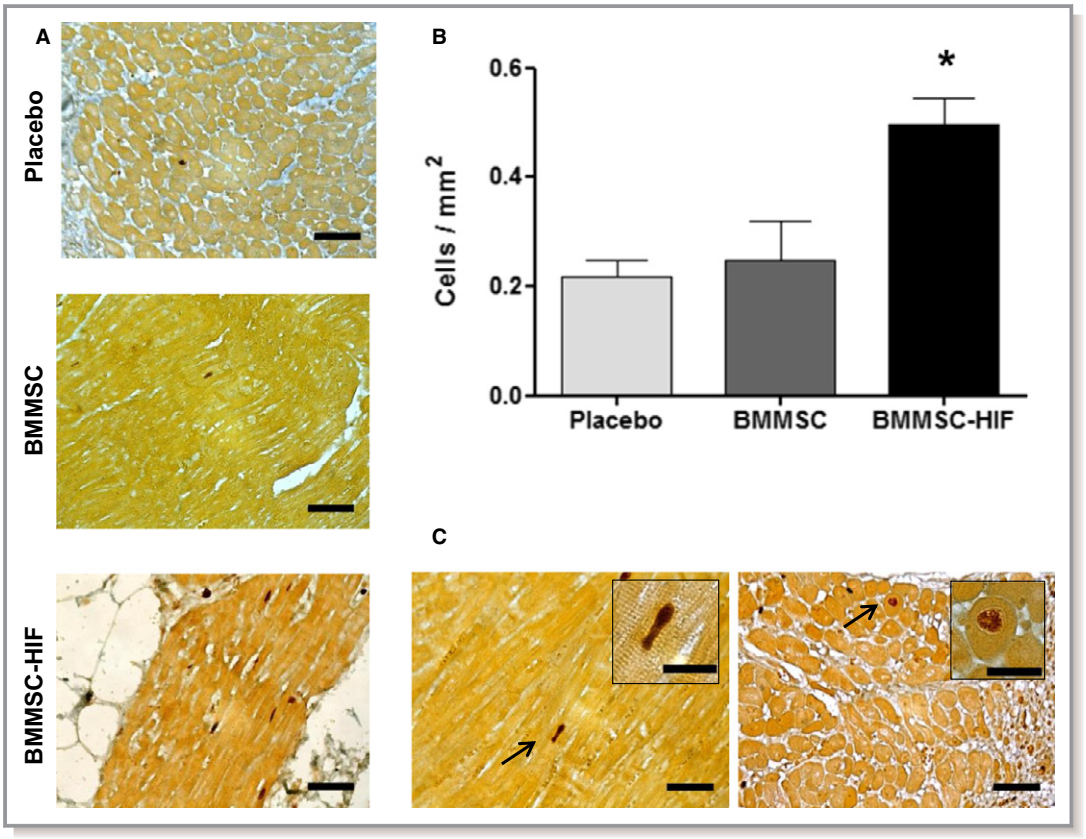

Figure 9. Anti-Ki67 staining of peri-infarct zones. A, Ki67-positive cardiomyocyte nuclei (stained brown) in Mallory-stained slices of the peri-infarct zone of a heart treated with placebo (upper), BMMSC (mid), and BMMSC-HIF (lower). Bars: 50 μm. B, Ki67-positive cardiomyocytes in treatment groups. **P*<0.05 vs placebo and BMMSC. C, Images of a heart treated with BMMSC-HIF at ×40 magnification (bars: 50 μm). Arrows indicate mitotic figures in adult cardiomyocytes nuclei, which are reproduced in the insets at ×100 magnification (bars: 20 μm). BMMSC: nontransfected bone marrow mesenchymal stromal cells. BMMSC-HIF: transfected BMMSC. HIF indicates hypoxia-inducible factor.

Nonetheless, further analysis based on their capacity to differentiate into adipocytes, chondrocytes, and osteocytes confirmed the mesenchymal nature of the cells. Likewise, the lack of ovine-specific antibodies prevented thorough characterization of secreted proteins that may be responsible for the cardioprotective effects observed in this study. As an alternative, we postulated that anti-human antibodies may be used to identify some of the secreted proteins. However, using a protein array spotted with human-specific, angiogenesis-related antibodies (ARY007; R&D Systems), only endothelin-1 and fibroblast growth factor were detectable (data not shown). As a consequence, this study is partially limited by a lack of thorough mechanistic insights in fully explaining the cardioprotective effects of modified MSCs, although we suspect increased neovascularization and reduced apoptosis as a consequence of released paracrine factors despite limited cell engraftment[43] to be important mediators.

Another limitation of the model is that it does not reproduce the risk factors and comorbidities usually associated with human ischemic heart disease. The findings that these features jeopardize the angiogenic efficiency of bone marrow cells[44] may help explain why clinical trials have failed to reproduce the therapeutic results obtained in animal models. Finally, a problem associated with the use of the intramyocardial route, namely, that part of the injectate is spilled back by systolic contraction, could be attenuated, but not prevented, by maintaining the needle in place for 30 seconds postinjection.

In summary, intramyocardial injection of allogeneic BMMSCs overexpressing a mutant, oxygen-resistant form of HIF1-α reduces infarct size and improves LV systolic performance to a significantly larger extent than BMMSCs in an ovine model of AMI. These effects are attributed to increased arteriolar proliferation and attenuated apoptosis induced by HIF-mediated overexpression of paracrine growth factors that also enhance long-term myocardial retention of injected cells. Given the excellent safety profile of the minicircle vector and feasibility of BMMSCs for allogeneic application, this treatment may be potentially useful in the clinic.

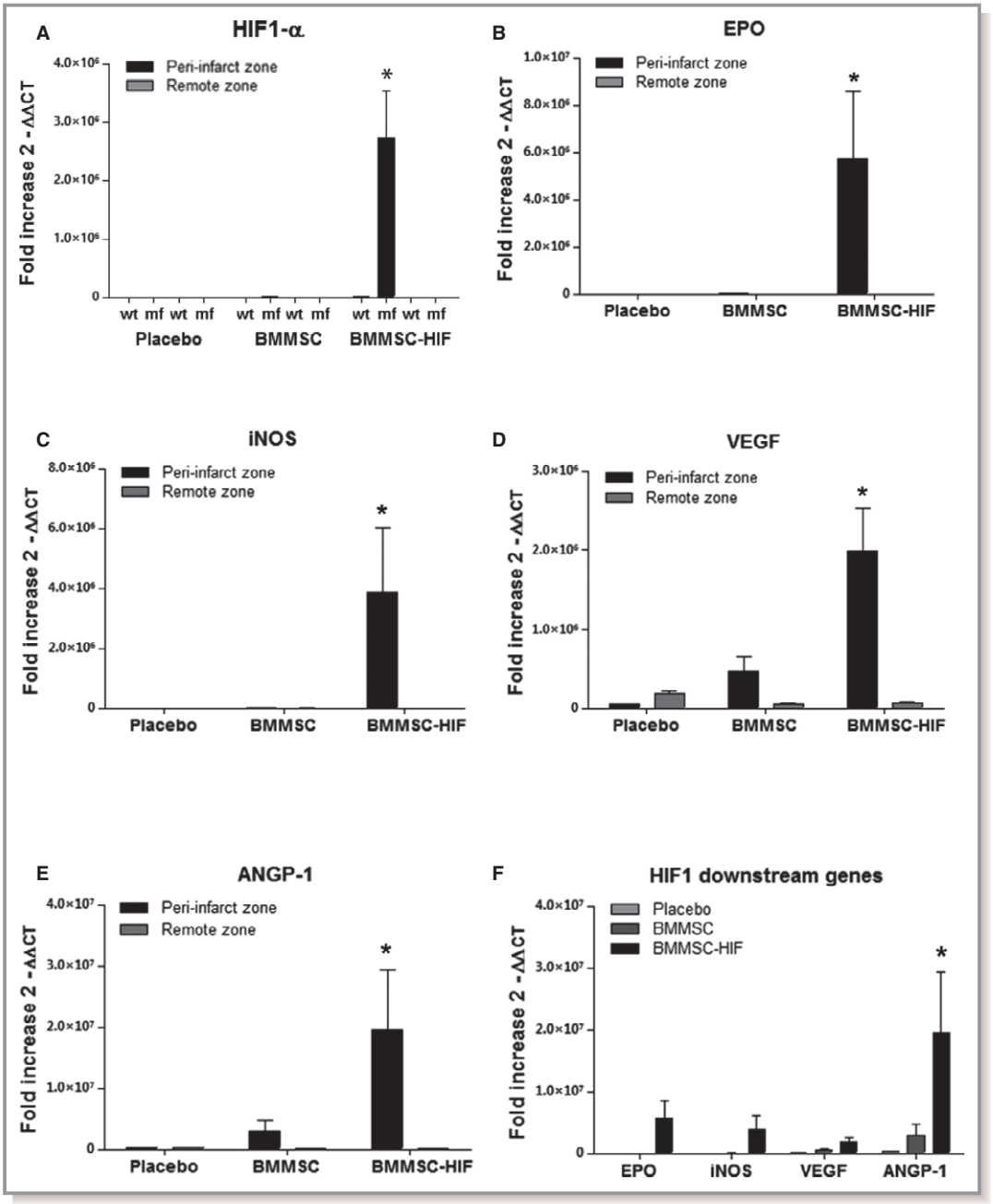

Figure 10. Gene expression at 7 days post-treatment. Expression of mutant form (mf) and wild-type form (wt) of HIF1-α (A), erythropoietin (EPO) (B), inducible nitrous oxide synthase (iNOS) (C), vascular endothelial growth factor (VEGF) (D), and angiopoietin-1 (ANGP-1) (E) genes in the peri-infarct and remote myocardium, indicating that, in all cases, gene expression is significantly higher in the peri-infarct zone of the BMMSC-HIF group. **P*<0.01 vs BMMSC and placebo. F, In the peri-infarct, ANGP-1 expression is higher than the other HIF1 downstream genes. **P*<0.001 vs EPO, iNOS, and VEGF. A, n=6 per group. B through F, n=4 per group. HIF indicates hypoxia-inducible factor.

Acknowledgments

We thank veterinarians María Inés Besansón and Pedro Iguain for anesthetic management and animal house assistants Juan Carlos Mansilla, Osvaldo Sosa, and Juan Ocampo for dedicated care of the animals. We also thank Julio Martínez, Fabián Gauna, Rosana Valverdi, and Leonardo Trejo for technical help.

Sources of Funding

This work was supported by grants PICT-PROBITEC 2011-2712 and PICT 2011-1181 from the National Agency for the Promotion of Science and Technology (ANPCyT), Ministry of Science, Technology and Innovative Production (MINCyT) of

Argentina, the René Barón Foundation of Argentina and the National Institutes of Health R01 HL093172 (Wu). We are grateful for the funding support by American Heart Association Postdoctoral Fellowship 15POST22940013 (Ong).

Disclosures

None.

References

1. World Health Organization. *Global Status Report on Noncommunicable Diseases 2014*. Geneva, Switzerland: WHO; 2014. Available at: http://www.who.int/nmh/publications/ncd-status-report-2014/en/. Accessed March 8, 2015.
2. Sutton MG, Sharpe N. Left ventricular remodeling after myocardial infarction: pathophysiology and therapy. *Circulation*. 2000;101:2981–2988.
3. English K. Mechanisms of mesenchymal stromal cell immunomodulation. *Immunol Cell Biol*. 2013;91:19–26.
4. Makino S, Fukuda K, Miyoshi S, Konishi F, Kodama H, Pan J, Sano M, Takahashi T, Hori S, Abe H, Hata J, Umezawa A, Ogawa S. Cardiomyocytes can be generated from marrow stromal cells in vitro. *J Clin Invest*. 1999;103:697–705.
5. Tang YL, Zhao Q, Qin X, Shen L, Cheng L, Ge J, Phillips MI. Paracrine action enhances the effects of autologous mesenchymal stem cell transplantation on vascular regeneration in rat model of myocardial infarction. *Ann Thorac Surg*. 2005;80:229–236.
6. Salem HK, Thiemermann C. Mesenchymal stromal cells: current understanding and clinical status. *Stem Cells*. 2010;28:585–596.
7. Lu F, Zhao X, Wu J, Cui Y, Mao Y, Chen K, Yuan Y, Gong D, Xu Z, Huang S. MSCs transfected with hepatocyte growth factor or vascular endothelial growth factor improve cardiac function in the infarcted porcine heart by increasing angiogenesis and reducing fibrosis. *Int J Cardiol*. 2013;167:2524–2532.
8. Semenza GL. Hypoxia-inducible factors in physiology and medicine. *Cell*. 2012;148:399–408.
9. Ivan M, Kondo K, Yang H, Kim W, Valiando J, Ohh M, Salic A, Asara JM, Lane WS, Kaelin WG Jr. HIFα targeted for VHL-mediated destruction by proline hydroxylation: implications for O_2 sensing. *Science*. 2001;292:464–468.
10. Kim CH, Cho YS, Chun YS, Park JW, Kim MS. Early expression of myocardial HIF-1 alpha in response to mechanical stresses: regulation by stretch-activated channels and the phosphatidylinositol 3-kinase signaling pathway. *Circ Res*. 2002;90:E25–E33.
11. Huang M, Chen Z, Hu S, Jia F, Li Z, Hoyt G, Robbins RC, Kay MA, Wu JC. Novel minicircle vector for gene therapy in murine myocardial infarction. *Circulation*. 2009;120:S230–S237.
12. Jia F, Wilson KD, Sun N, Gupta DM, Huang M, Li Z, Panetta NJ, Chen ZY, Robbins RC, Kay MA, Longaker MT, Wu JC. A nonviral minicircle vector for deriving human iPS cells. *Nat Methods*. 2010;7:197–199.
13. Yun Z, Lin Q, Giaccia AJ. Adaptive myogenesis under hypoxia. *Mol Cell Biol*. 2005;25:3040–3055.
14. Keeney M, Ong SG, Padilla A, Yao Z, Goodman S, Wu JC, Yang F. Development of poly (β-amino esters)-based biodegradable nanoparticles for non-viral delivery of minicircle DNA. *ACS Nano*. 2013;7:7241–7250.
15. Ong SG, Lee WH, Huang M, Dey D, Kodo K, Sanchez-Freire V, Gold JD, Wu JC. Cross talk of combined gene and cell therapy in ischemic heart disease: role of exosomal microRNA transfer. *Circulation*. 2014;130:S60–S69.
16. Ong SG, Lee WH, Theodorou L, Kodo K, Lim SY, Shukla DH, Briston T, Kiriakidis S, Ashcroft M, Davidson SM, Maxwell PH, Yellon DM, Hausenloy DJ. HIF-1 reduces ischaemia-reperfusion injury in the heart by targeting the mitochondrial permeability transition pore. *Cardiovasc Res*. 2014;104:24–36.
17. Riegler J, Cheung KK, Man YF, Cleary JO, Price AN, Lythgoe MF. Comparison of segmentation methods for MRI measurement of cardiac function in rats. *J Magn Reson Imaging*. 2010;32:869–877.
18. Amado LC, Saliaris AP, Schuleri KH, St John M, Xie JS, Cattaneo S, Durand DJ, Fitton T, Kuang JQ, Stewart G, Lehrke S, Baumgartner WW, Martin BJ, Heldman AW, Hare JM. Cardiac repair with intramyocardial injection of allogeneic mesenchymal stem cells after myocardial infarction. *Proc Natl Acad Sci USA*. 2005;102:11474–11479.
19. Liu C, Fan Y, Zhou L, Zhu HY, Song YC, Hu L, Wang Y, Li QP. Pretreatment of mesenchymal stem cells with angiotensin II enhances paracrine effects, angiogenesis, gap junction formation and therapeutic efficacy for myocardial infarction. *Int J Cardiol*. 2015;188:22–32.
20. Locatelli P, Olea FD, Mendiz O, Salmo F, Fazzi L, Hnatiuk A, Laguens R, Crottogini A. An ovine model of postinfarction dilated cardiomyopathy in animals with highly variable coronary anatomy. *ILAR J*. 2011;52:E16–E21.
21. Kinnaird T, Stabile E, Burnett MS, Lee CW, Barr S, Fuchs S, Epstein SE. Marrow-derived stromal cells express genes encoding a broad spectrum of arteriogenic cytokines and promote in vitro and in vivo arteriogenesis through paracrine mechanisms. *Circ Res*. 2004;94:678–685.
22. Ranganath SH, Levy O, Inamdar MS, Karp JM. Harnessing the mesenchymal stem cell secretome for the treatment of cardiovascular disease. *Cell Stem Cell*. 2012;10:244–258.
23. Rahbarghazi R, Nassiri SM, Ahmadi Mohammadi E, Rabbani S, Araghi A, Hosseinkhani H. Dynamic induction of pro-angiogenic milieu after transplantation of marrow-derived mesenchymal stem cells in experimental myocardial infarction. *Int J Cardiol*. 2014;173:453–466.
24. Locatelli P, Olea FD, Hnatiuk A, De Lorenzi A, Cerdá M, Giménez CS, Sepúlveda D, Laguens R, Crottogini A. Mesenchymal stromal cells overexpressing vascular endothelial growth factor in ovine myocardial infarction. *Gene Ther*. 2015;22:449–457.
25. Cerrada I, Ruiz-Saurí A, Carrero R, Trigueros C, Dorronsoro A, Sanchez-Puelles JM, Diez-Juan A, Montero JA, Sepúlveda P. Hypoxia-inducible factor 1 alpha contributes to cardiac healing in mesenchymal stem cells-mediated cardiac repair. *Stem Cells Dev*. 2013;22:501–511.
26. Bai CG, Liu XH, Liu WQ, Ma DL. Regional expression of the hypoxia-inducible factor (HIF) system and association with cardiomyocyte cell cycle re-entry after myocardial infarction in rats. *Heart Vessels*. 2008;23:193–200.
27. Hu X, Xu Y, Zhong Z, Wu Y, Zhao J, Wang Y, Cheng H, Kong M, Zhang F, Chen Q, Sun J, Li Q, Jin J, Li Q, Chen L, Wang CH, Zhan H, Fan Y, Yang Q, Yu L, Wu R, Liang J, Zhu J, Wang Y, Jin Y, Lin Y, Yang F, Jia L, Zhu W, Chen J, Yu H, Zhang J, Wang J. A large-scale investigation of hypoxia-preconditioned allogeneic mesenchymal stem cells for myocardial repair in nonhuman primates: paracrine activity without remuscularization. *Circ Res*. 2016;118:970–983 doi: 10.1161/CIRCRESAHA.115.307516. Epub January 19, 2016.
28. Laguens R, Cabeza Meckert P, Vera Janavel G, De Lorenzi A, Lascano E, Negroni J, Del Valle H, Cuniberti L, Martínez V, Dulbecco E, Melo C, Fernández N, Criscuolo M, Crottogini A. Cardiomyocyte hyperplasia after plasmid-mediated vascular endothelial growth factor gene transfer in pigs with chronic myocardial ischemia. *J Gene Med*. 2004;6:222–227.
29. Vera Janavel G, Crottogini A, Cabeza Meckert P, Cuniberti L, Mele A, Papouchado M, Fernández N, Bercovich A, Criscuolo M, Melo C, Laguens R. Plasmid-mediated VEGF gene transfer induces cardiomyogenesis and reduces myocardial infarct size in sheep. *Gene Ther*. 2006;13:1133–1142.
30. Ferrarini M, Arsic N, Recchia FA, Zentilin L, Zacchigna S, Xu X, Linke A, Giacca M, Hintze TH. Adeno-associated virus-mediated tansduction of VEGF165 improves cardiac tissue viability and functional recovery after permanent coronary occlusion in conscious dogs. *Circ Res*. 2006;98:954–961.
31. Malliaras K, Marbán E. Cardiac cell therapy: where we've been, where we are, and where we should be headed. *Br Med Bull*. 2011;98:161–185.
32. Hou D, Youssef EA, Brinton TJ, Zhang P, Rogers P, Price ET, Yeung AC, Johnstone BH, Yock PG, March KL. Radiolabeled cell distribution after intramyocardial, intracoronary, and interstitial retrograde coronary venous delivery: implications for current clinical trials. *Circulation*. 2005;112:I150–I156.
33. Gyöngyösi M, Hemetsberger R, Posa A, Charwat S, Pavo N, Petnehazy O, Petrasi Z, Pavo IJ, Hemetsberger H, Benedek I, Benedek T, Benedek I Jr, Kovacs I, Kaun C, Maurer G. Hypoxia-inducible factor 1-alpha release after intracoronary versus intramyocardial stem cell therapy in myocardial infarction. *J Cardiovasc Transl Res*. 2010;3:114–121.
34. Peng C, Yang K, Xiang P, Zhang C, Zou L, Wu X, Gao Y, Kang Z, He K, Liu J, Cheng M, Wang J, Chen L. Effect of transplantation with autologous bone marrow stem cells on acute myocardial infarction. *Int J Cardiol*. 2013;162:158–165.
35. Amsalem Y, Mardor Y, Feinberg MS, Landa N, Miller L, Daniels D, Ocherashvilli A, Holbova R, Yosef O, Barbash IM, Leor J. Iron-oxide labeling and outcome of transplanted mesenchymal stem cells in the infarcted myocardium. *Circulation*. 2007;116:I38–I145.
36. Drey F, Choi YH, Neef K, Ewert B, Tenbrock A, Treskes P, Bovenschulte H, Liakopoulos OJ, Brenkmann M, Stamm C, Wittwer T, Wahlers T. Noninvasive in vivo tracking of mesenchymal stem cells and evaluation of cell therapeutic effects in a murine model using a clinical 3.0 T MRI. *Cell Transplant*. 2013;22:1971–1980.
37. Loor G, Schumacker PT. Role of hypoxia-inducible factor in cell survival during myocardial ischemia-reperfusion. *Cell Death Differ*. 2008;15:686–690.

38. Jones SP, Bolli R. The ubiquitous role of nitric oxide in cardioprotection. *J Mol Cell Cardiol*. 2006;40:16–23.

39. Azarnoush K, Maurel A, Sebbah L, Carrion C, Bissery A, Mandet C, Pouly J, Bruneval P, Hagège AA, Menasché P. Enhancement of the functional benefits of skeletal myoblast transplantation by means of coadministration of hypoxia-inducible factor 1alpha. *J Thorac Cardiovasc Surg*. 2005;130:173–179.

40. Kiani AA, Kazemi A, Halabian R, Mohammadipour M, Jahanian-Najafabadi A, Roudkenar MH. HIF-1α confers resistance to induced stress in bone marrow-derived mesenchymal stem cells. *Arch Med Res*. 2013;44:185–193.

41. Hamamoto H, Gorman JH III, Ryan LP, Hinmon R, Martens TP, Schuster MD, Plappert T, Kiupel M, St John-Sutton MG, Itescu S, Gorman RC. Allogeneic mesenchymal precursor cell therapy to limit remodeling after myocardial infarction: the effect of cell dosage. *Ann Thorac Surg*. 2009;87:794–802.

42. Houtgraaf JH, de Jong R, Kazemi K, de Groot D, van der Spoel TI, Arslan F, Hoefer I, Pasterkamp G, Itescu S, Zijlstra F, Geleijnse ML, Serruys PW, Duckers HJ. Intracoronary infusion of allogeneic mesenchymal precursor cells directly after experimental acute myocardial infarction reduces infarct size, abrogates adverse remodeling, and improves cardiac function. *Circ Res*. 2013;113:153–166.

43. Ong SG, Huber BC, Lee WH, Kodo K, Ebert AD, Ma Y, Nguyen PK, Diecke S, Chen WY, Wu JC. Microfluidic single-cell analysis of transplanted human induced pluripotent stem cell-derived cardiomyocytes after acute myocardial infarction. *Circulation*. 2015;132:762–771.

44. Heeschen C, Lehmann R, Honold J, Assmus B, Aicher A, Walter DH, Martin H, Zeiher AM, Dimmeler S. Profoundly reduced neovascularization capacity of bone marrow mononuclear cells derived from patients with chronic ischemic heart disease. *Circulation*. 2004;109:1615–1622.